Spring 2018

Quantifying Sedimentation Patterns of Small Watersheds in the Central Oregon Coast Range Using Landslide-Dammed Lakes

Logan Wetherell
Central Washington University, logan.wetherell@cwu.edu

QUANTIFYING SEDIMENTATION PATTERNS OF SMALL WATERSHEDS IN THE CENTRAL OREGON COAST RANGE USING LANDSLIDE-DAMMED LAKES

A Thesis

Presented to

The Graduate Faculty

Central Washington University

In Partial Fulfillment

of the Requirements for the Degree

Master of Science

Geology

by

Logan Reed Wetherell

May 2018

CENTRAL WASHINGTON UNIVERSITY

Graduate Studies

We hereby approve the thesis of

Logan R. Wetherell

Candidate for the degree of Master of Science

APPROVED FOR THE GRADUATE FACULTY

______________ ______________________________
Dr. Lisa L. Ely, Committee Chair

______________ ______________________________
Dr. Megan K. Walsh

______________ ______________________________
Dr. Joshua J. Roering

______________ ______________________________
Dean of Graduate Studies

ABSTRACT

QUANTIFYING SEDIMENTATION PATTERNS OF SMALL WATERSHEDS IN THE CENTRAL OREGON COAST RANGE USING LANDSLIDE-DAMMED LAKES

by

Logan Reed Wetherell

May, 2018

Up to 250 years of sedimentation patterns in headwater streams are preserved with detail in landslide-dammed lakes of the central Oregon Coast Range. I hypothesize that both anthropogenic and natural perturbations should increase linear and mass sediment accumulation rates and be discernible spatially and temporally in the sediment record with use of ^{137}Cs, high resolution charcoal stratigraphy, and aerial photography. Klickitat Lake and Wasson Lake are landslide-dammed lakes in small watersheds (<10 km^2) that contain drowned Douglas-fir stumps that are used for accurate dendrochronology and precise timing of the lake formation. An age-depth relationship was developed using ^{137}Cs and identifiable fire events, which demonstrates that each lake has high linear sedimentation accumulation rates (0.2 – 4.5 cm y^{-1}) and variable mass accumulation rates. Both lakes exhibit similar changes in mass and sediment accumulation, with rates remaining low after formation of each landslide-dammed lake and stabilizing after the initial lake filling. Stand-replacing wildfires of the mid-19th century increased short- and long-term sedimentation and mass accumulation rates, but they are not a primary driver in sediment mobilization and deposition. Sedimentation to the lakes systematically and gradually increased after the 1920s. Rates peaked in the mid-20th century associated with above-average peak discharge events with wetter and cooler conditions across the Pacific Northwest. Sediment deposition to the repositories has since decreased, but remains elevated compared to pre-industrial logging and road development. Comparisons to other landslide-dammed sediment repositories in the region suggest higher sedimentation rates in the steeper southern Tyee Formation, and lower sediment mobilization potential in the deep-seated dominated northern Tyee Formation. Results of this study indicate that small landslide-dammed lakes are viable tools for assessing sediment mobility patterns in headwater channels and can be used to further understand sedimentation and erosional patterns in the central Oregon Coast Range.

ACKNOWLEDGMENTS

I would first like to thank my entire thesis committee in being wonderful advisors focused on advancing science in a fun, realistic, and enjoyable manner. To my primary advisor, I would like to thank Dr. Lisa Ely for always having a positive outlook on all variables surrounding my thesis and for always having the door open to her office to deal with my spontaneous epiphanies. A large thanks to Dr. Megan Walsh and her REU students Keifer Nace and Molly Burchfield for being an immense help in collecting and analyzing my cores, and for being wonderfully entertaining in the lab. I would like to also extend a special thanks to Dr. Josh Roering for encouraging me as a spastic undergraduate to migrate into the field of geomorphology and for his continual help in my path to becoming a professional geologist.

Finally, I must express deep gratitude to my wife and best friend Meaghan Wetherell for pushing me through my thesis and reminding me that anxiety is normal. This accomplishment would not have been possible without her. Thank you.

Logan Reed Wetherell

TABLE OF CONTENTS

TABLE OF CONTENTS CONTINUED

LIST OF TABLES

LIST OF FIGURES

LIST OF FIGURES CONTINUED

Figure Page

LIST OF FIGURES CONTINUED

Figure Page

Chapter I
INTRODUCTION

Landslide-dammed lakes in watersheds of the Oregon Coast Range (OCR) act as sediment repositories, preserving stochastic erosional processes and allowing researchers to quantify changes in sedimentation patterns of individual basins (e.g. Worona and Whitlock, 1995; Long, 1998; Richardson, 2018). Larger landslide-dammed lakes in higher-order streams (e.g. Triangle Lake, Loon Lake) have been the focus of many sedimentological and paleoecological studies, but smaller landslide-dammed lakes have not been considered in earlier research. First and second-order streams where small landslide dams originate, represent 60-90% of cumulative channel length in mountainous terrain and are one of the direct pathways for directing water, sediment, and wood from hillslopes to higher-order river systems in the OCR (Schumm, 1956; Shreve, 1969; Benda and Dunne, 1997; May and Gresswell, 2002). Many of these low-order coastal streams provide critical channel structure for anadromous salmon and resident fish species that have declined over the last century due to ecological changes in spawning habitat (Nehlsen et al., 1991). Anthropogenic erosional activities such as logging and roadbuilding have been suggested as a primary factor in the decline of fish; these practices can clog stream channels with fine particulates that choke salmon eggs, decrease stream habitat quality and lower invertebrate populations (Brown and Krygier, 1971; Beschta 1978).

The relationship between basin-wide natural and anthropogenic perturbations (e.g. wildfires, floods, logging) and sediment yield is poorly defined in small watersheds

(<10 km^2) because of short measurement periods and inherent spatial and temporal variability in erosional processes (Reneau and Dietrich, 1990). Sediment transport and influx to channel networks is characteristically stochastic and difficult to quantify because they are driven by precipitation and other perturbations that are discrete in space and time (Benda and Dunne, 1997; Lancaster et al., 2001, Lancaster and Casebeer, 2007). Because of these geomorphic, environmental and social issues associated with sedimentation in salmon-rearing streams, it is important to understand the variability of natural and anthropogenic perturbations in small watersheds and the contribution of sedimentation from individual events in streams systems of the OCR. Few studies have documented and quantified historic linear sedimentation and mass accumulation rates (SAR; MAR) of landslide-dammed lakes in headwater streams and their response to anthropogenic disturbances and major precipitation and climatic changes. Given the evidence of recurring fires in the mountainous central OCR (e.g. Impara, 1997; Zybach, 2003), these landslide-dammed lakes also offer a unique opportunity to observe the fire-driven effects on sediment accumulation within isolated watersheds.

The purpose of this study is to assess the significance of natural and anthropogenic perturbations to erosion and sedimentation patterns within small watersheds in the central OCR over the last several centuries. The goals of this project are to; (1) quantify sedimentation rates within the Klickitat and Wasson Lake watersheds beginning with their formation and landslide-damming origin, (2) assess changes in sedimentation patterns after the catastrophic fires of the 19th century, (3) evaluate changes in sedimentation with deviations in regional climate affecting precipitation and flood regimes, (4) assess fluctuations in sediment accumulation rates from onset of anthropogenic perturbations such as road building and logging, and (5) qualitatively determine the stability of the landslide dams by identifying lake-level fluctuations via preservation of submerged ghost forests.

The results of this study can be applied toward deciphering the stochastic nature of sediment mobilization in forested headwater streams from episodic disturbances that are generated by both anthropogenic and natural sources. Because small streams make up a large percentage of the total stream length in the OCR, understanding temporal fluctuations in sediment transport is important for quantifying the total sediment budget of major watersheds that provide salmon-spawning habitat and supply sediment to the depositional sinks of large oceanic deltas (Lancaster and Grant, 2006).

1.1 Background

Landslide-dammed lakes occurring within the Tyee Formation of the central Oregon Coast Range are ideal for studying decadal-scale sedimentation rates from natural and anthropogenic sources due to the near-homogenous lithology, minimal tectonic deformation of the Tyee Formation, and lack of Pleistocene glaciation across the range (Reneau and Deitrich, 1991; Heimsath et al., 2001). Bedrock in the central OCR is dominated by the Middle Eocene Tyee Formation and composed of approximately 3 km of predominantly massive arkosic and greywacke marine sandstone and siltstone turbidite deposits derived from plutonic and metamorphic sources from the Klamath Mountains and the Idaho Batholith (Heller et al., 1985) (Figure 1). At least 13 natural lakes within the Tyee Formation are derived from landslides of mostly unknown ages (Figure 2). Many of the landslide-dammed lakes act as sediment repositories that are ideal sites for studying sediment yield and climatic effects on coastal range watersheds by capturing in-transit sediment and organic debris within the watershed (e.g. Worona and Whitlock, 1995; Long et al., 1998). However, little is known about the stability, longevity, or morphological effects of the dams in low-order drainages (Lane, 1987).

Because of their significant size, the sediment repositories associated with Oregon estuaries and large landslide-dammed lakes reflect important long-term climatic and ecological data (e.g. Long et al., 1998; Wheatcroft et al., 2013; Marshall et al., 2017; Richardson, 2017). These widely dispersed watersheds record variability in late Holocene sedimentation events and are useful for defining earthquake, climate, and anthropogenic perturbations. In these large watersheds, difficulty arises in detecting the effects of individual perturbations on small watersheds typical of the OCR.

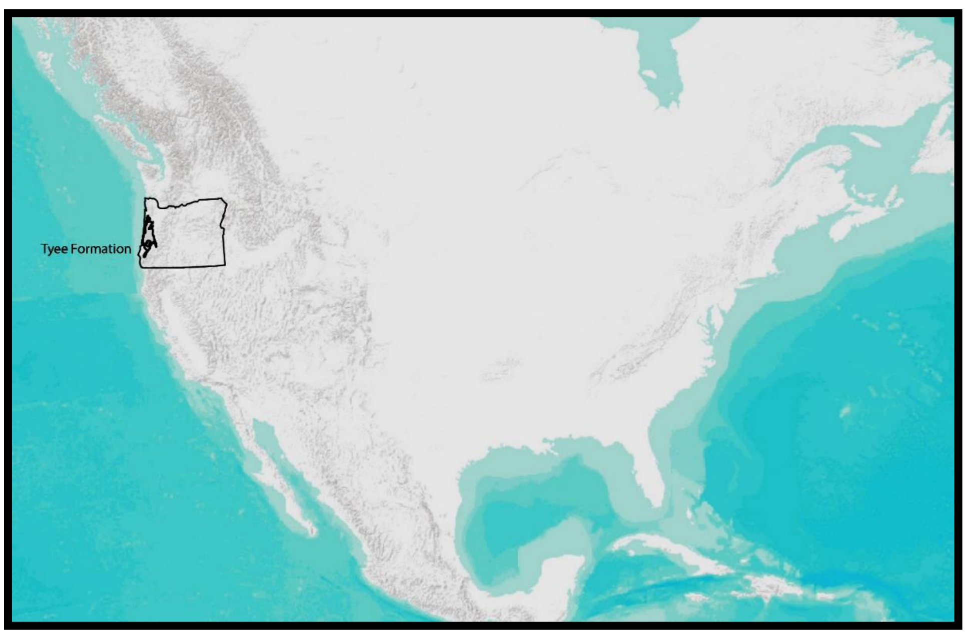

Figure 1. Overview of North America and location of the Tyee Formation and Oregon Coast Range within western Oregon.

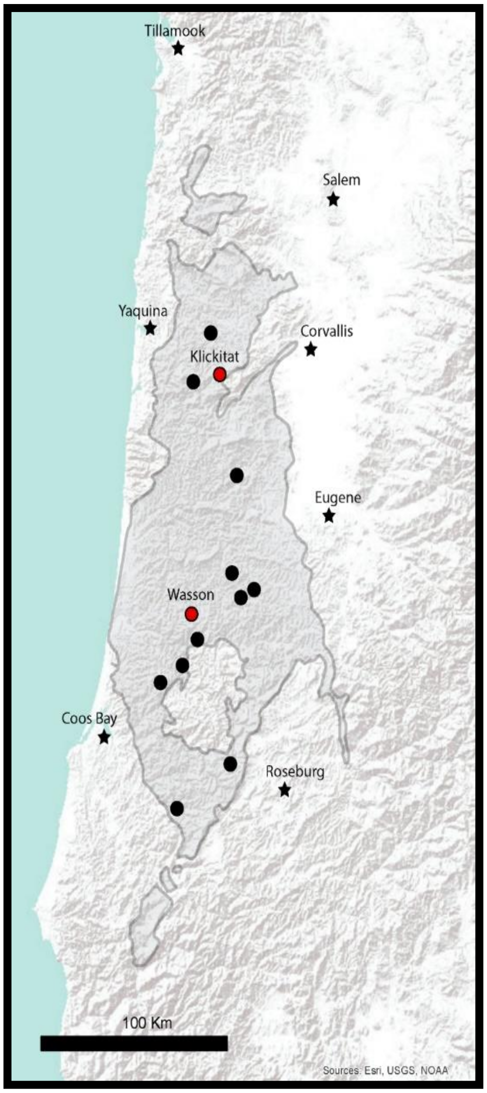

Figure 2. Boundaries of the Tyee Formation and location of landslide-dammed lakes within the central OCR labelled with black circles. Lake sites cored for this study are labelled in red.

This study suggests that small and mountainous landslide-dammed lakes can be exploited for understanding the temporal and spatial distribution of sediment pulses and the influence of natural and anthropogenic perturbations in the immediately adjacent small streams and hillslopes. The novel approach of using small landslide-dammed lakes to quantify sedimentation patterns in headwater streams of the OCR has not been tested before due to access difficulties, complex basin morphology, and lack of temporal markers within the stratigraphy

Geology and Physiography

The central OCR is primarily composed of the middle Eocene Tyee Formation (Snavely et al., 1964) (Figure 2). The Tyee Formation is approximately 3-km thick and is composed of turbidite deposits derived from terrestrial plutonic and metamorphic sources from the Klamath Mountains and the Idaho Batholith (Snavely et al., 1964; Heller et al., 1985). This prograding delta-fed submarine ramp system rapidly deposited several kilometers of sediments before rotating >50° after the Eocene as the coastline of

Oregon rapidly migrated westward approximately 100 km (Lovell 1969; Chan and Dott, 1983; Heller et al., 1985). Because the Tyee Formation developed on a large deltaic system feeding from a major river out of the Klamath Mountains, the southern formation is dominated by massive sandstone turbidites up to 10 m in thickness and lesser amounts of siltstone interbeds, while the northern Tyee Formation contains thinner sandstone beds with increasing to equal amounts of siltstone (Chan and Dott, 1983; Roering, 2005). Material larger than granule or pebble-sized is uncommon in the Tyee Formation except in the far south where conglomeratic lenses occur in some thick sandstone units, however, no general relationship is apparent between bed thickness and maximum grain size (Hoover, 1963; Snavely et al., 1964). Turbidite deposits within the Tyee Formation are thickest near the base with the underlying Umpqua Group, which is deposited on the Early Eocene accreted seamount terrane of Siletzia (Snavely et al., 1964; Heller and Ryberg, 1983).

In the OCR, drainages and hillslopes are often steep due to the uniform bedrock and topography, with slopes approaching 50° in some basins. Hillslope morphology is composed of convex ridge tops dominated by soil creep, while small soil slip and shallow landslides dominate the steep sideslopes (Dietrich and Dunne, 1987; Roering et al., 1999). Soils can extend to depths near 10 m on ridgetops but rapidly thin or becomes absent on slopes (Swanston and Swanson, 1976; Dietrich and Dunne, 1987).

Differences in volume of siltstone interbeds affect the style of mass-wasting and relief of topography in the Tyee Formation (Roering, 2005). Higher amounts of siltstone in the northern Tyee Formation result in abundant deep-seated landslides that fail with dip direction, while denudation of the southern extent of the formation is dominated by debris flows and fluvial incision (Roering, 2005).

Over millennial timescales, the central OCR is proposed to approximate steady-state uplift and erosion owing to the prevalence of steep, uniform topography and relatively uniform measurements of erosion rates from cosmogenic nuclides (e.g. Bierman et al., 2001; Heimsath et al., 2001; Kelsey et al., 1996; Personius, 1995; Reneau and Dietrich, 1991). Terraces uplift records indicate uplift rates averaging 0.1 to 0.3 mm y^{-1} since the Miocene (Kelsey et al., 1996), whereas short and long-term (>10,000 y) hillslope erosion rates commonly range from 0.05 to 0.3 mm y^{-1} (Reneau and Dietrich, 1991; Heimsath et al., 2001; Penserini, 2015; Marshall and Roering, 2014). These variable results suggest hillslope erosion rates fluctuate over short (i.e. human) timescales, but when averaged over thousands of years the landscape appears to be eroding at roughly the same rate of 0.1 to 0.2 mm y^{-1} (Heimsath et al., 2001).

Sediment Supply

Sediment accumulation in landslide-dammed lakes and other sediment repositories are dependent on the relationship between sediment supply from erosional perturbations and the transport capacity of fluvial networks (Sklar and Dietrich, 1998; Hancock and Anderson, 2002; Lancaster and Casebeer, 2007). Rapid sediment production can occur within a basin but may not be locally reflected in the sedimentary record if that material is not immediately transported and deposited (Benda and Dunne, 1990). This lag between erosion and deposition could create discrepancies between sedimentation and hillslope erosion, especially in complex low-order streams of the OCR.

Debris flows are the primary erosive driver connecting hillslopes to alluvial channels in low-order basins (Dietrich and Dunne, 1978; Swanson et al., 1982; Benda, 1990). In the OCR, debris hollows accumulate sediment and organics from centuries to few thousand years before it is rapidly released in mass movement events (May and Gresswell, 2003). Once soil and organic debris is released from the debris channels, it is then deposited at the base of the slope as a colluvial wedge and debris dam awaiting transport as sediment in the stream (Lancaster and Grant; 2006; Lancaster and Casebeer, 2007). Transit times of sediment from the debris deposit varies, but is on the order hundreds to few thousands of years as much of the coarse gravels and boulders derived from the debris flow are not mobilized by most peak discharge events (Lancaster and Grant, 2006).

Deposits of colluvium and coarse organics accumulate within unchanneled valleys (hollows) near the boundary of low-order channels and are stationary until pore pressure from large precipitation events surpasses root strength, and wedges of colluvium are evacuated from the hillside in the form of shallow landslides that often transform into debris flows (May and Gresswell, 2003). The frequency of debris flow passage depends on location in the valley network as downstream locations have more potential upstream landslide sources and thus tend to experience more frequent debris flow activity.

Fire History

Verbal and written wildfire accounts for the OCR date to the mid-18th century with increases in recorded events beginning with the large catastrophic and stand-replacing fires in the mid-19th century. Compiled diaries and verbal accounts passed down by Native Americans provide a 250+ year wildfire history, and when coupled with studies of burn scars (e.g. Impara, 1997), provide an extensive chronology for fire events for the region (Zybach, 2003). Large catastrophic fires of the mid-19th century (e.g. Yaquina I Fire, 1849; Coos Fire, 1868) likely played a significant role in the settlement of more remote reaches of in the densely vegetated interior OCR, and also affected the future distribution of private and public timber lands.

The Oregon Department of Forestry was established in 1911 and marked the onset of wildfire mitigation across the state. In 1933, the first Tillamook Burn occurred, burning over 1200 km^2 of timberland across northwestern Oregon (Morris, 1935). During the following period, forest roads and lookout towers were constructed rapidly by the Civilian Conservation Corps work crews to reduce damage from fires across the region (Zybach, 2003). Several more reburn events occurred within and outside of the original Tillamook Burn with the last related wildfire occurring in 1951. By this period, fire prevention, advancements in aerial firefighting, and access to remote regions of the interior coast range substantially decreased fire activity with very few wildfires occurring between 1951 and 1987 (Oregon Department of Forestry, 2018). A dry summer in 1987 resulted in large fires burning over 400 km^2 and in 2002, the Biscuit Fire burned over 2000 km^2 (Oregon Department of Forestry, 2018) Since the start of the

21^{st} century, fires in southwestern Oregon covering over 40 km^2 have occurred almost biennially (Zybach, 2003, Oregon Department of Forestry, 2018).

Wildfires and Sediment Mobilization

The relationship between fire and increased mass-wasting has been observed in the OCR with a >40% increase in debris flows in the decades immediately following a wildfire (e.g. May and Gresswell, 2002; Roering and Gerber, 2005). Counteracting the increase in mass wasting, a rapid increase in wood within the stream after fires increases the sediment storage potential of channels, retaining most entrained material (May and Gresswell, 2002). This may lead to a longer period of increased sedimentation but with less intensity, mitigating the increase in hillslope erosion.

Measurements and simulations of sediment production suggest that fire-related processes account for approximately 50% of temporally averaged sediment yield in steep regions (Roering and Gerber, 2005). Post-fire erosion has been observed in the OCR with colluvial transport occurring via dry ravel, and the emergence of bedrock and talus-like slopes from excessive transport of soil from steep slopes (Jackson and Roering, 2009). The ignition of vegetation dries soil horizons, which exacerbates dry raveling and reduces root strength for the following decade. This loss of vegetation increases the likelihood for filled colluvial hollows to form shallow landslides during succeeding rain events, with additional debris flows spawned by the mobilization of fire-related sediment and organics that have accumulated in valley bottoms (Cannon et al., 2001). These observations also suggest that the rates of sediment transport and erosion associated with wildfires can exceed long-term rates by an order of magnitude or greater, potentially making fires a dominant cause of erosion (Wilson et al., 2001; Roering and Gerber, 2005).

Anthropogenic Disturbances

Fire regimes of western Oregon were greatly affected by the devastation of Native American populations prior to the mid-19th century. The onset of American expansion to the west introduced diseases by fur traders that decimated most native populations by the mid-19th century, and many trail networks subsequently collapsed (Zybach, 2003).

After the removal of indigenous peoples, initial road development in the OCR occurred along major waterways connecting the Willamette and Umpqua Valley to the ocean (Watson, 1951). The introduction of gasoline engines and the post-World War II economic boom led to abundant road building operations in the mid-20th century, with new road networks developed across previously inaccessible terrain (Hoyt, 1966). Early roadbuilding methods were not designed to minimize erosion and sedimentation to stream systems, and roads were often constructed hastily with hillslope colluvium removed via bulldozer and logged tree roots often used as road-fill.

The Oregon Forest Practices Act in 1971 was the first course of legal action developed in the United States around timber harvest techniques to protect natural resources and public interests (Ice et al., 1997). This act set initial standards for the building and maintaining of roads, along with changes in forest harvest practices and the replacing of harvested trees. Modifications to the Oregon Forest Practices Act over the last few decades have strengthened rules to prevent erosion to hillsides and roads. In place are regulations minimizing exposure time of heavy equipment and logging in the heavy precipitation winter months and implement streamside buffer zones to protect water quality (Ice et al., 1997). These changes from earlier logging methods have been successful when measuring sedimentation in estuaries and large watersheds with many contributing stream systems (e.g. Wheatcroft, 2013; Richardson, 2017); however, the success of the Oregon Forest Practices Act and its effect on sedimentation rates have not been measured in small landslide-dammed lakes high in watersheds.

1.2 Study sites

Klickitat Lake and Wasson Lake in the central OCR and were chosen based on access to submerged stumps for dendrochronology, drainage morphology representative of typical basins in the OCR, and records of historic land use in the contributing watersheds (Figure 3). The two lakes have similar drainage areas that are characteristic of headwater channels. Klickitat Lake is larger (4 ha), with a drainage area of 6.7 km^2 and is located in the north-central OCR. Wasson Lake (1.6 ha) has a drainage area of 3.0 km^2 and is in the south-central OCR between the Smith and Umpqua Rivers.

Klickitat Lake, Oregon (44.4800° Lat., -123.6590° Long., 360 m a.s.l.), is located approximately 10 km north of Alsea and 9 km southwest of Mary’s Peak, the highest point in the Oregon Coast Range. The lake was formed by a deep-seated landslide in AD 1751 that originated from a north-facing slope with the toe of the slide making a 120° eastward bend downstream during the wasting event (Figure 4) (W. Struble and B. Black, personal communication, October 2017).

In addition, two small debris channels across the stream from the toe of the landslide appear to have failed at unknown times and potentially added additional sediment to the downstream toe of the landslide. The Klickitat Lake watershed covers 6.7 km^2 , and Lake Creek and Klickitat Creek are the two major tributaries that feed into the lake. Several other small perennial streams feed into Klickitat Lake, but appear to have minimal effect on sediment deposition based on lack of substantial prograding deltas in the bathymetry. LiDAR data indicate wide deltas from Lake and Klickitat Creeks extending up to 0.5 km upstream from the current shore line. These deltas, together with evidence of lake-level change on drowned stumps, suggest that the lake was close to 10 ha in surface area at maximum lake height. In March 2017, Klickitat Lake had a maximum depth of 4.5 m and average basin depth near 4 m (Figure 5). A regularly used forest road is located on the eastern and northern shores of Klickitat Lake, as lake is a recreational site for fisherman and is a main route for timber harvest transport.

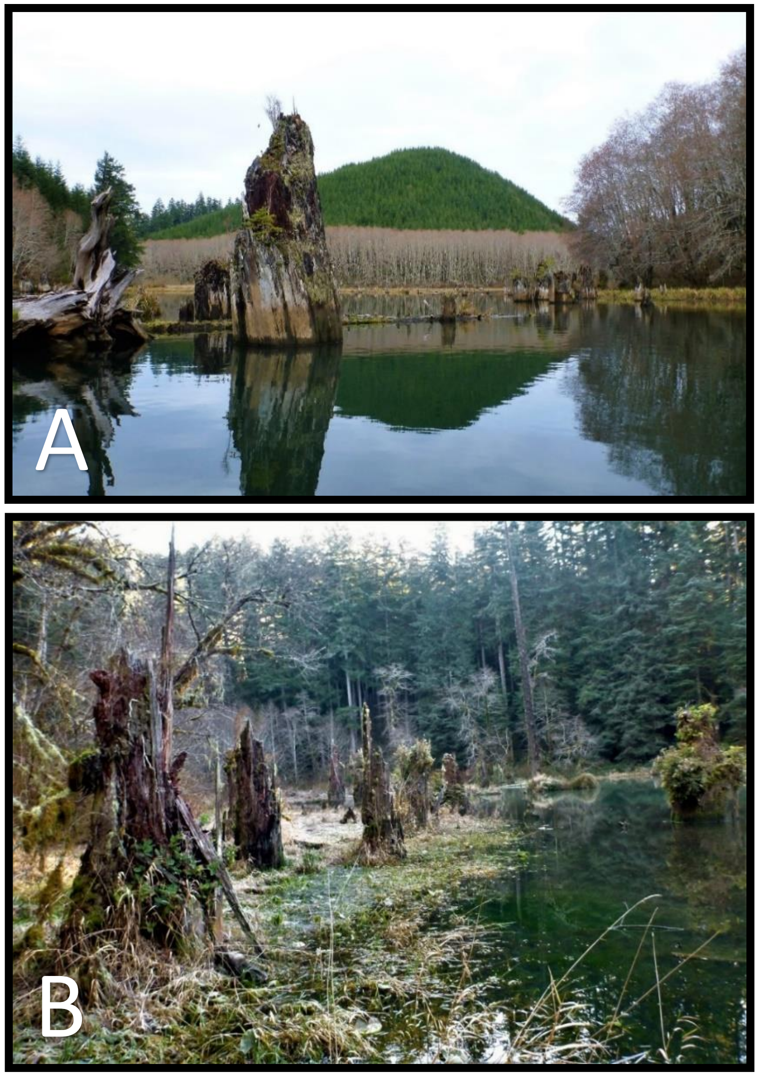

Figure 3. Stands of partially submerged Douglas-fir ghost forests in Klickitat (A) and Wasson Lake (B). Average diameter of Douglas-fir trees in each lake range from 1-2 m, with Klickitat Lake having noticeably larger and better preserved stumps. Note "bathtub" rings evident on trees within Klickitat Lake compared to weathered stumps in Wasson Lake.

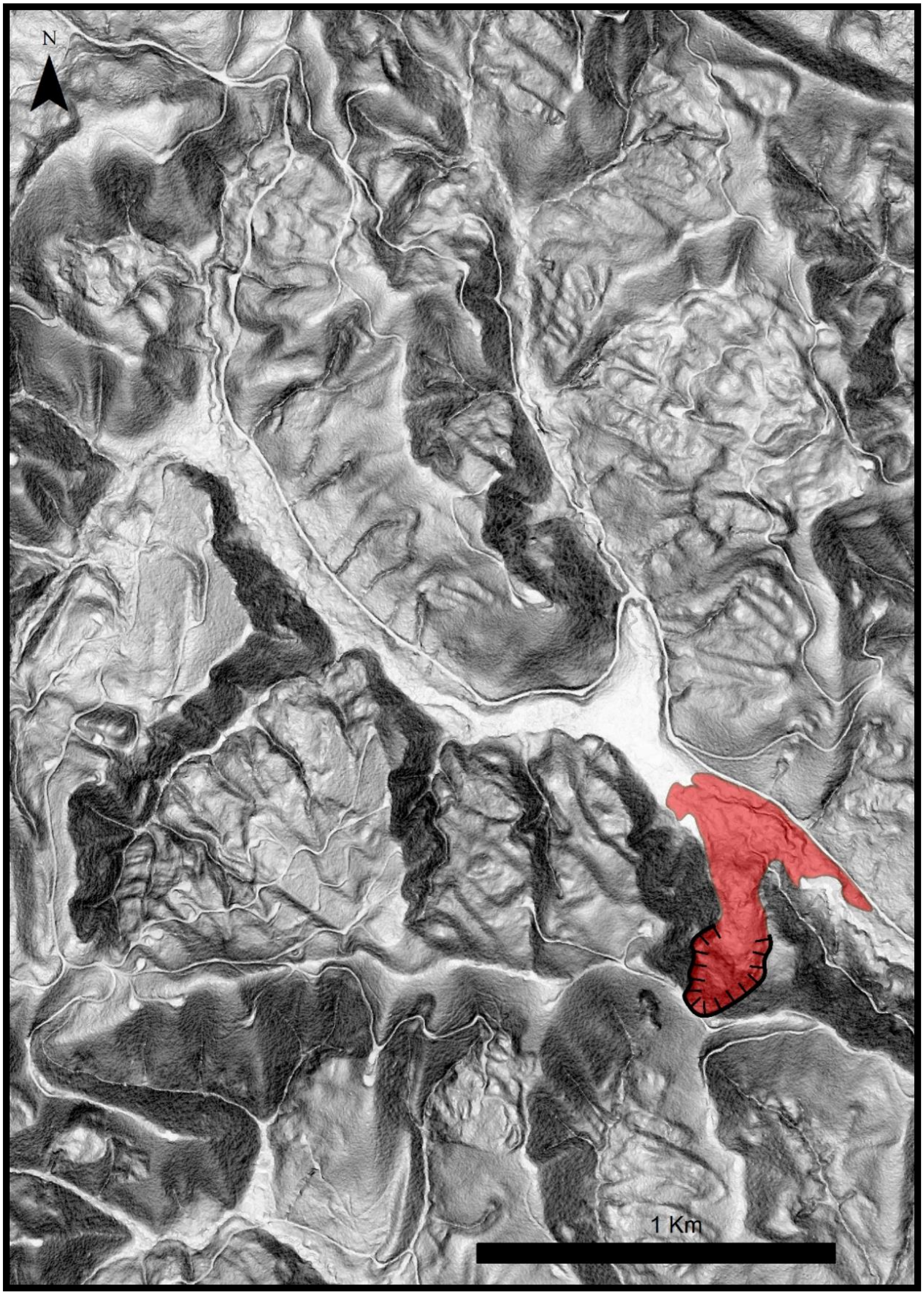

Figure 4. LiDAR derived hillslope image of Klickitat Lake with landslide and landslide-dam material in red. Note hummocky and irregular topography on many slopes in the basin.

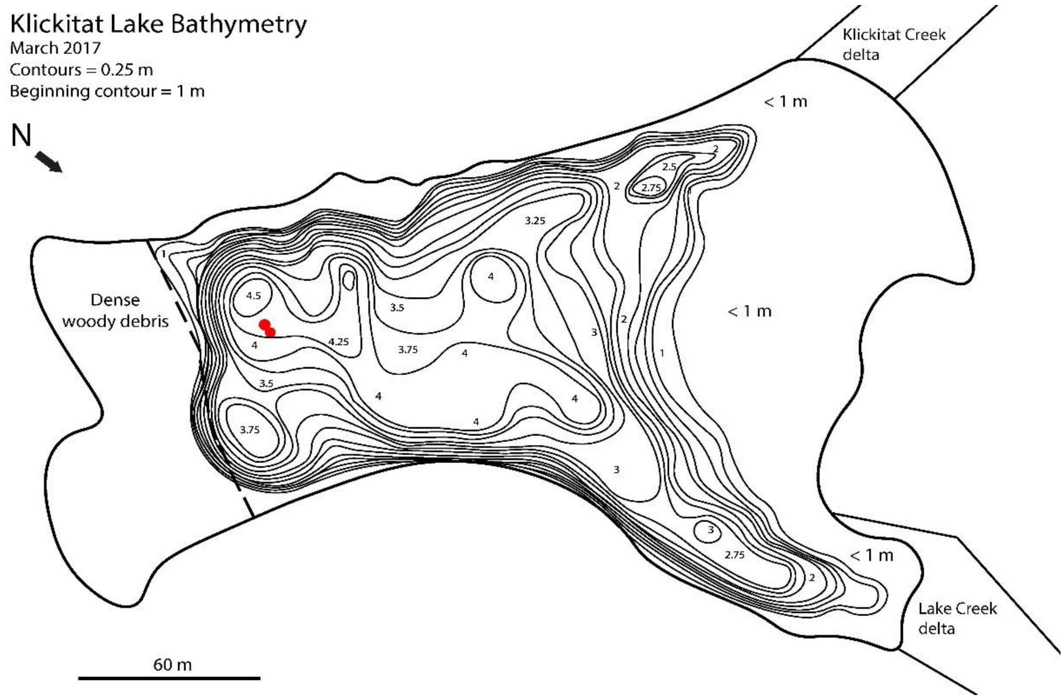

Figure 5. Klickitat Lake bathymetry with coring site indicated by red dots. Lake floor is more irregular than Wasson Lake but the maximum depths are the same.

The Klickitat Lake watershed is owned by federal and private timber companies and is dominated by second- and third-growth with few old-growth *Pseudotsuga menziesii* (Douglas-fir). In the immediate vicinity of the lake, *Alnus rubra* (red alder) grows along the shore and in debris hollows, and *Acer macrophyllum* (big leaf maple) is located on the forest road with lesser amounts of *Sambucus racemose* (red elderberry). Shrubs found near Klickitat Lake include *Rubus spectabilis (*salmonberry), *Gaultheria shallon* (salal), *Rubus armeniacus* (himalayan blackberry), *Spiraea douglasii* (hardhack) and *Vaccinium ovalifolium* (oval-leaf blueberry). Growing within the margins of the lake are *Typha spp.* (cattail), *Nurphar polysepala* (yellow water lily), along with *Lysichiton americanus* (skunk cabbage).

Wasson Lake (also known as Wassen), Oregon (43.7477° Lat., -123.7956° Long., 230 m a.s.l.), is located 82 km due south of Klickitat Lake and is approximately 10 km north of Scottsburg and the Umpqua River. The 1.6 ha lake formed from a shallow landslide in 1819 (Figure 6) (W. Struble and B. Black, personal communication, October 2017), that blocked Wasson Creek, which flows into the Smith River 26 km downstream. The bulk of the landslide deposit covers 2.5 ha and originated on north facing slopes blocking both the headwaters of Wasson Creek and an unnamed perennial stream. In March 2017, the maximum lake level was 4.5 m deep near the western shore and landslide-dam, while the average lake bottom was 4 to 4.25 m deep (Figure 7). The prograding delta at Wasson Creek is steep and drops quickly into the lake, while the unnamed creek contains a more gently sloped prograding delta. Two other ephemeral streams do not appear to have a significant influence on sediment deposition based on bathymetry and lack of significant deltas.

Wasson Lake is surrounded by second-growth forest of *Pseudotsuga menziesii*, which dominates the landscape, with lesser amounts of *Tsuga heterophylla* in the understory. *Alnus rubra* is abundant near the lake along with *Salix* spp.and *Acer macrophyllum*, which is found growing along roads. Growing within openings in the canopy are *Rubus spectabilis*, *Rubus parviflorus*, *Gaultheria shallon*), *Polystichum munitum* (swordfern), *Berberis aquifolium* (Oregon grape), and lesser amounts of *Pteridium aquilinum* (bracken fern), *Vaccinium parvifolium* (huckleberry), *Acer circinatum* (vine maple), and less *Dryopteris expansa* (spiny wood fern) and a few *Sambucus racemose* (red elder berry). Herbaceous plants include *Oxalis oregana* (sorrel), *Digitalis purpurea* (foxglove), and other grasses. The most abundant aquatic plants observed include *Nurphar polysepala*. Wasson Lake appears to have very few recreational visitors, but an overgrown trail and campsite is present near a primitive boat launch directly across from the landslide dam suggesting occasional fishing use.

Multiple Chinook salmon (*Oncorhynchus tshawytscha*) have been observed spawning and in the final stages of life nearby at Yellow Lake (20 km east) and Gould Lake (26 km south), both landslide-generated lakes in the Tyee Formation. Sand-rich sediment and stable water levels potentially make these isolated lakes ideal salmon habitat with abundant coarse organics for rearing of hatched fry. Online fishing forums suggest that cutthroat trout (*Oncorhynchus clarkia*) are also present at Klickitat and Wasson Lakes.

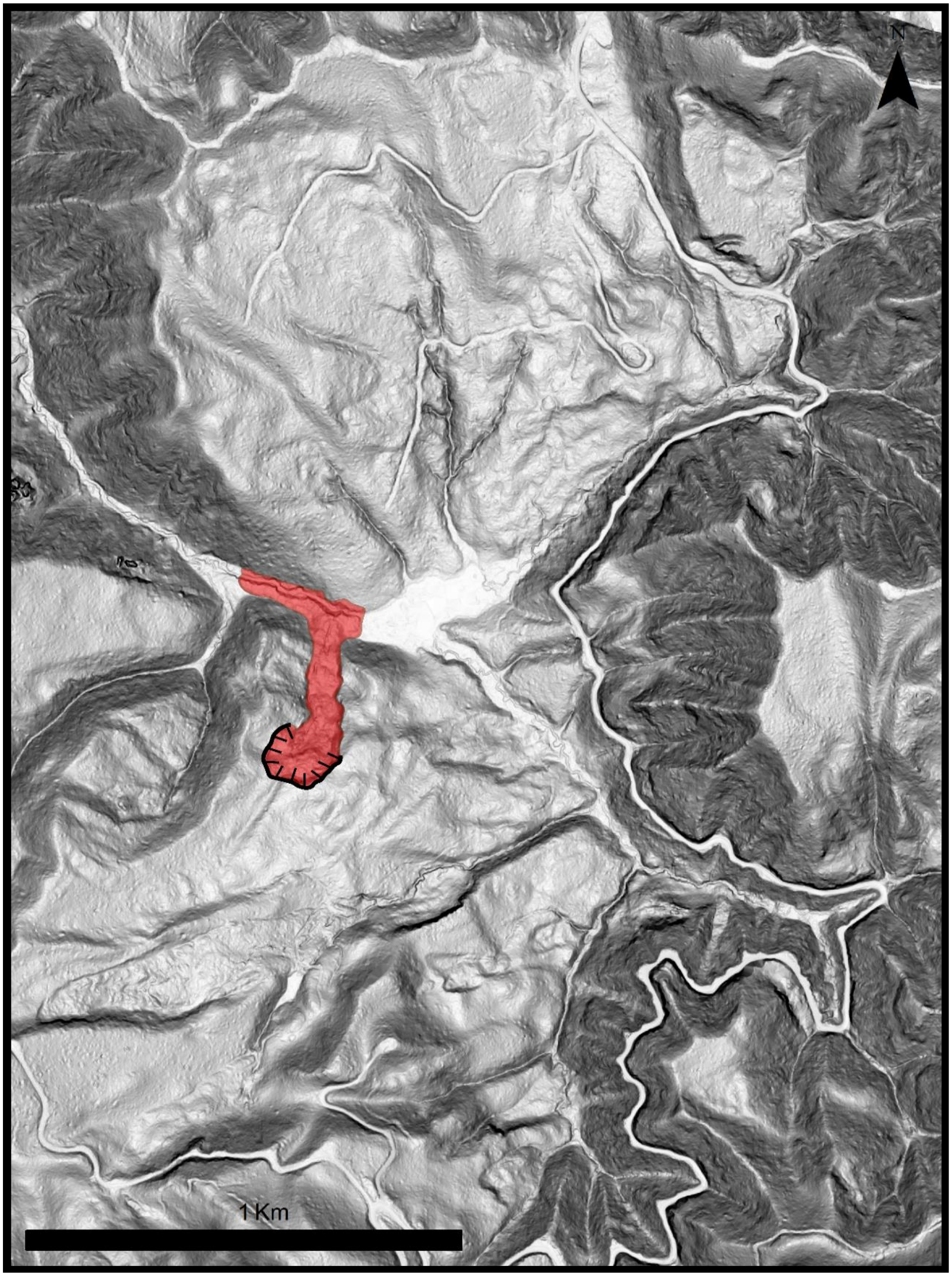

Figure 6. LiDAR derived hillslope image of Wasson Lake watershed with landslide and landslide-dam material in red. Another earthflow and landslide-dammed marsh on a lower-order drainage is present approximately 0.5 km south of the landslide scarp.

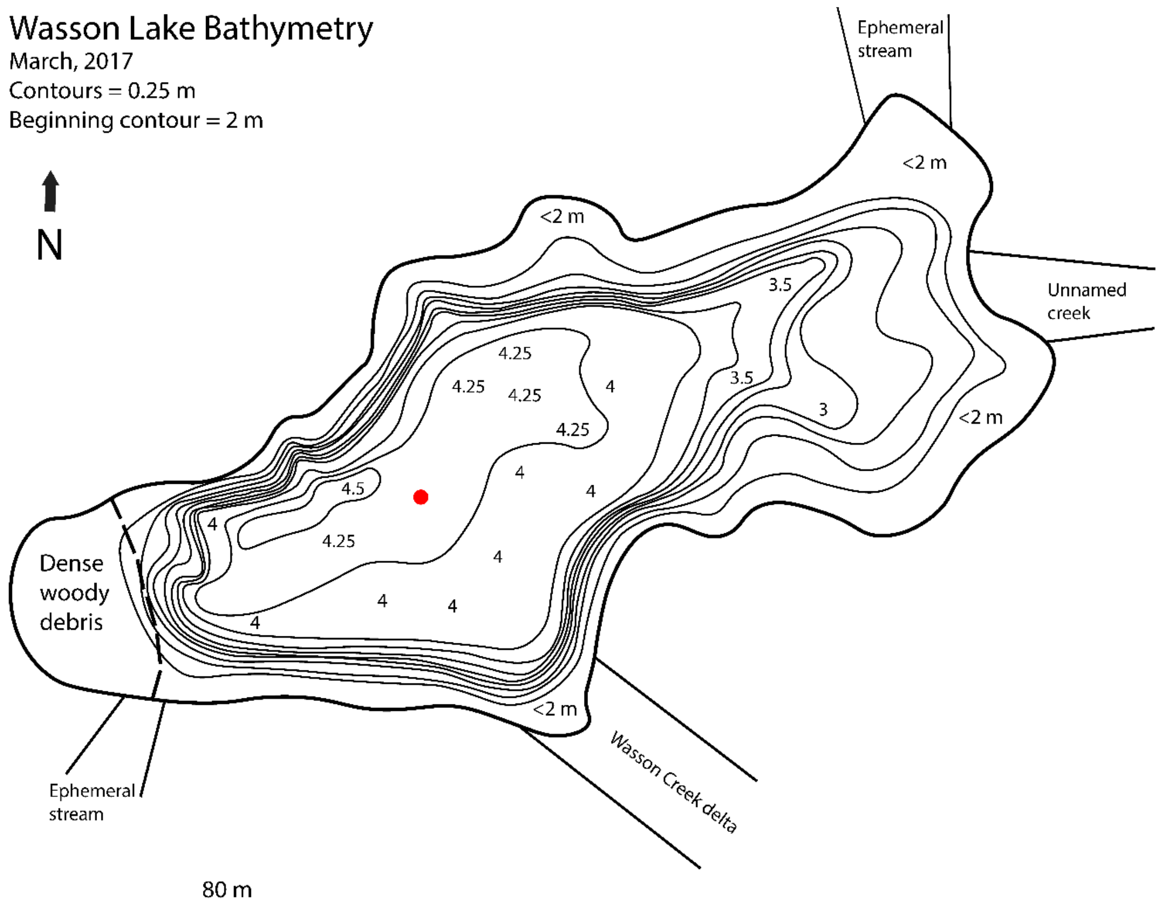

Figure 7. Wasson Lake bathymetry with coring site indicated by red dot. Lake bottom is consistently flat with steep shorelines except along the northeast deltas. The front of the Wasson Creek delta drops off rapidly, suggesting that the delta is prograding rapidly.

Climate and Hydrologic Data

The central Oregon Coast Range is a 60 to 80 km wide belt of steep, soil-mantled, and heavily vegetated terrain with average relief of 450 m and elevation ranging from sea level to 1,241 m at Mary's Peak. The marine west-coast climate for the region is characterized by cool, wet winters and warm, dry summers with 1-2 m of annual precipitation falling as rain between October and April and minimal snow occurring at higher elevations (McGarigal and McComb, 1995). At the Fish Creek fish hatchery near the Alsea River, 11 km south of Klickitat Lake, average annual temperature is 11°C (51°F) and receives 2280 mm of annual rainfall (Figure 8). In the southeastern part of the research area at Elkton, 20 km south of Wasson Lake, average annual temperatures are 12° C (54°F) and mean precipitation is substantially less at Elkton with 1260 mm of total precipitation as rainfall (Western Regional Climate Data, 2017) (Figure 9).

Peak annual stream flow data were collected from USGS National Water Information System from four central OCR rivers with the longest continual records. Stream data from the Umpqua River at Elkton and Siletz River at Siletz, provided the longest records, beginning in 1906 and 1917, respectively. Data from the South Fork of the Coquille and Alsea River provided additional context for the magnitude of flood events in the central OCR. The Umpqua River is the largest drainage examined and is heavily affected by snow melt from the Cascade Range, while the remainder have headwaters in the coast range. For the Umpqua River at Elkton, discharge records indicate an average annual peak discharge near 2900 $m^3 s^{-1}$ with peak discharge occurring in the winter of 1964/65 with a velocity of 7500 $m^3 s^{-1}$. Other notable flood events with peak discharges 1.5 times greater than average occurred in 1927, 1943, 1946, 1951, 1954, 1956, 1961, 1971, 1974, 1982, 1996, 2006, and 2012 (Figure 10). Hydrograph data from major central coast rivers indicate extremely low discharge years occurring in 1917, 1931, 1935, 1977, 1992, and 2001 but these do not appear to be associated with peaks in average temperatures. Periods of low discharge are consistent across the central coast range.

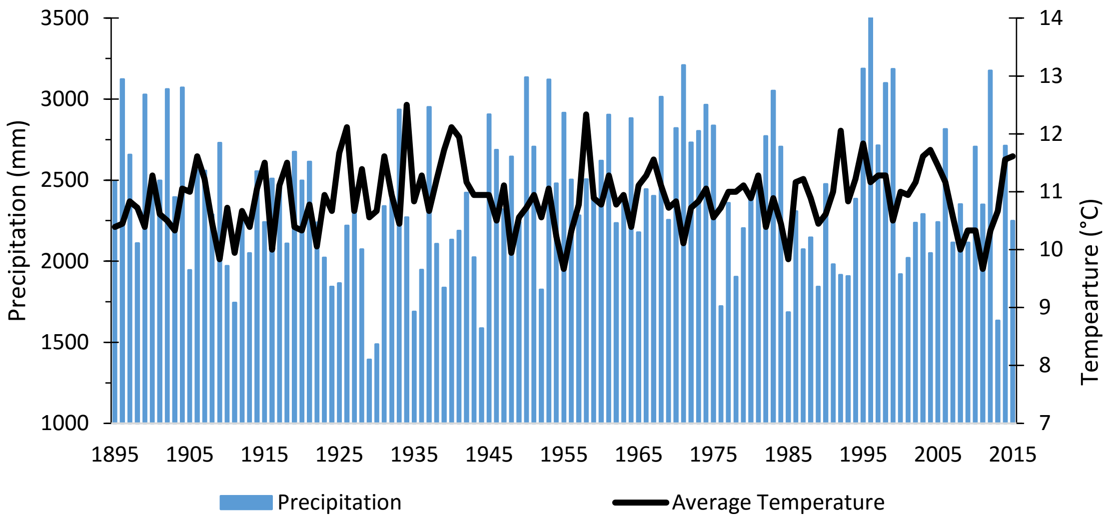

Figure 8. Modelled annual precipitation and average temperature near Klickitat Lake. Annual climate data produced by PRISM Climate Group by calculating a climate-elevation regression for each local DEM grid cell and nearby weather stations (Daly et al., 2008). Source: PRISM Climate Group, 2018.

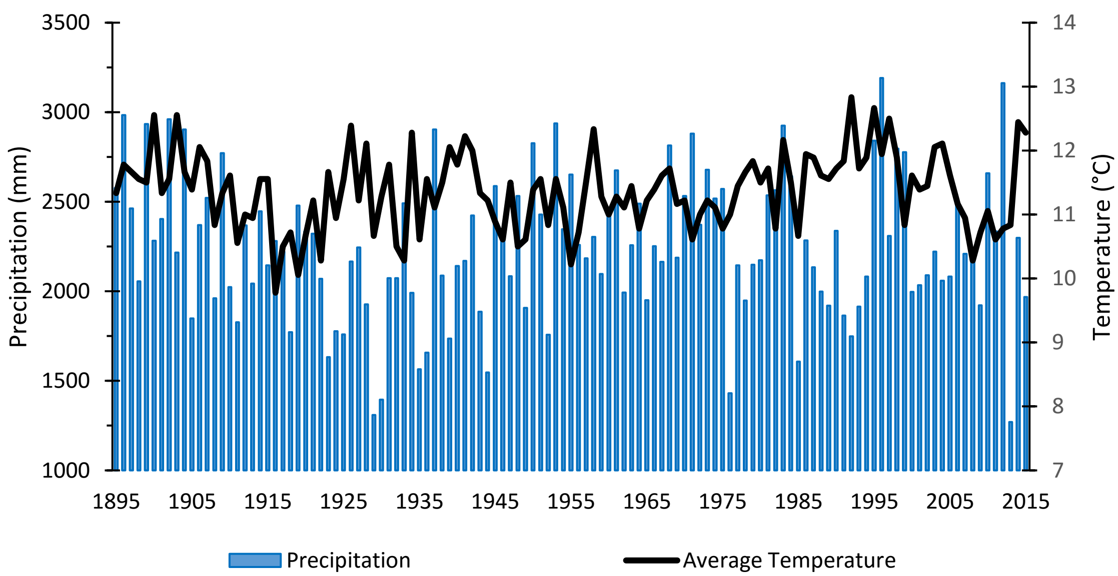

Figure 9. Modelled annual precipitation and average temperatures for Wasson Lake watershed. Source: PRISM Climate Group, 2018.

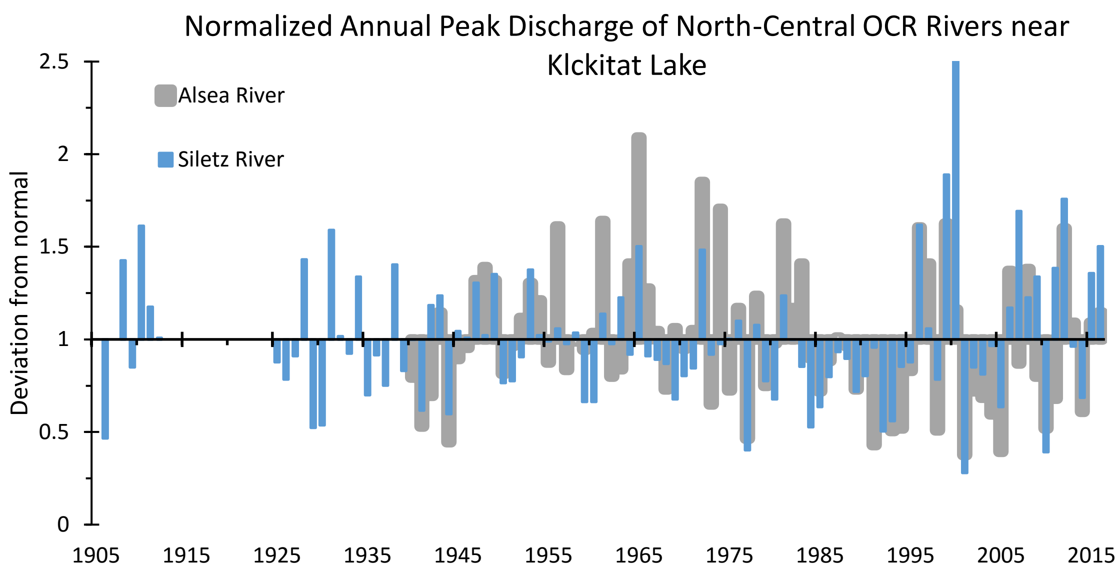

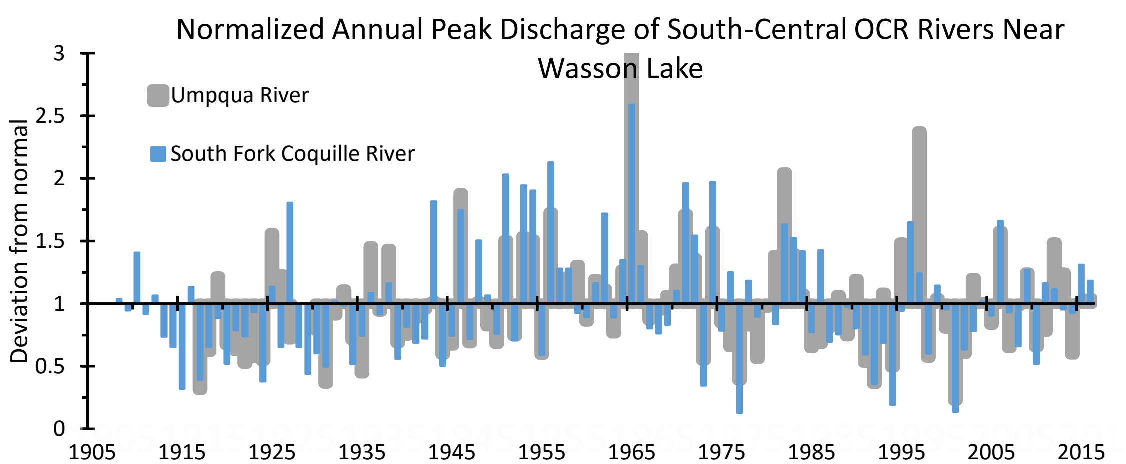

Figure 10. Normalized annual peak discharge of rivers near Klickitat and Wasson Lakes with longest continuous records. Most peak discharge events are distributed across the range with the 1964/65 floods producing the highest discharge events.

Chapter II

METHODS

2.1 Coring and Sedimentary Analysis

Prior to coring, I gathered coarse resolution lake bathymetry from a raft using a secci disk to identify ideal sediment coring locations and provide qualitative information about the lake basin morphology (Figure 11). At a later time, we collected sediment from each lake using a 5-cm diameter modified Livingstone piston corer and 7-cm diameter Bolivia piston corer (Wright et al., 1987). The top 20 cm of sediment from the sediment-water interface was subsampled into 1 cm intervals and stored in Whirl-Pak bags. The remainder of the core was extruded and wrapped in plastic wrap and aluminum foil and secured in PVC casing. Sediment was immediately wrapped and transported to Dr. Megan Walsh's Paleoecology Lab at Central Washington University and stored at 2°C.

In Wasson Lake, we collected sediment from one location (WAS17A) near the landslide dam and edge of the floating log mats. We collected cores from the sediment-water interface until reaching the saprolite of the Tyee Formation. At Klickitat Lake, we collected from two locations directly adjacent to each other. KL17A contains 61 cm of sediment and was stopped by submerged wood. The coring site was moved horizontally approximately 2 m and a second series of continuous cores were extracted using a Livingstone Corer until the saprolite was reached. A distinct marker bed was identified at 52 cm depth in both KL17A and KL17B and was used to correlate these cores together into a single stratigraphic sequence. Material from 52 cm to 61 cm in KL17A was discarded to minimize stratigraphic contamination (i.e. modification of local depositional patterns from the submerged wood).

I dissected cores longitudinally, photographed, and described stratigraphy using standard lithostratigraphic analysis. The color of individual beds was identified using a Munsell Soil Chart. Small terrestrial plant macrofossils (e.g. needles, leaves, small twigs) were identified in the basal lacustrine sediments and sent for ^{14}C-AMS dating to confirm the general time frame of the dendrochronology ages of each lake (W. Struble and B. Black, personal communication, October 2017).

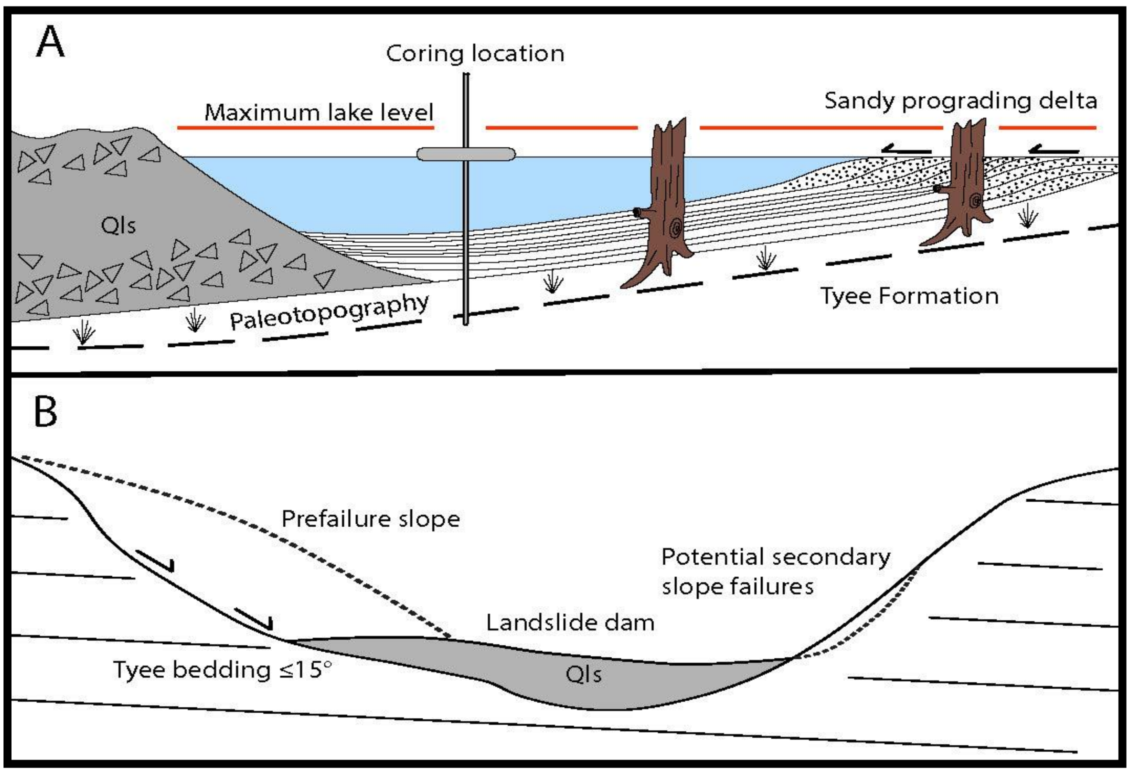

Figure 11. A) Idealized landslide-dammed lake and coring location minimizing sedimentary disturbances from oscillations in delta progradation. Coarse organics complicate coring as many stumps and logs are buried in sediment and out of view.

B) Typical landslide-dammed lake formation and shallow secondary slope failures. In general, landslides fail in the direction of dip of the bedrock bedding with debris flows being the most common mechanism of failure on slopes against dip. Modified from Lane (1987), and Roering (2005).

I analyzed grain size of the lake sediment and underlying stream deposits using a Malvert Mastersizer 3000 Hydro LV laser diffraction particle size analyzer with a refractive index of 1.457, adsorption index of 0.01, and density of 1.0 g/cm^3. Samples were prepared by first dehydrating 1 cm increments at 65^0 C for several days. Approximately 1-2 cm^3 of sediment from each sample were next disaggregated and processed, gently rehydrated and added to Hydro LV unit with ultrasonic treatment until 15-30% laser obscuration within deionized water was reached. Three grain-size measurements were calculated for each 1 cm increment and grain-size averages were recorded.

Loss-on-ignition determines the bulk density, organic, and carbonate content of sediment (Dean, 1974) and was completed by Dr. Megan Walsh and NSF Research Experience for Undergraduate (REU) students. The team extracted 1 cm^3 of wet sediment at 2 cm intervals for the length of the cores. Samples were dried at 90°C overnight to provide a dry density of the sediment and organics. Samples were next heated to 550°C for 2 hours and then at 900°C for 2 hours with weight taken after each combustion. Changes in weight after each burn determined the dry mass and percentage of organic and carbonate content in each sample. A multiplication factor of 1.36 was applied to the loss at 900°C to determine the carbonate content (Dean, 1974).

Magnetic susceptibility determines changes in allochthonous inorganic content of the core and helps to identify changes in sedimentation (Thompson and Oldfield, 1986). I measured intact cores using a Sapphire Instruments, 5 cm wide magnetic coil on each core at contiguous 1 cm intervals to compare changes in electromagnetic units with changes in grain size, charcoal, loss-on-ignition, and sedimentation rates.

Charcoal is an inert inorganic compound that results from incomplete combustion of plant tissues (Patterson et al., 1987). Local charcoal is deposited dominantly via fluvial transport by stream systems following fires but can also be dispersed by aeolian transport from distant events (Blong and Gillespie, 1978; Rummery, 1983; Patterson et al., 1987; Whitlock and Larsen, 2002). Transport time for local events is shortest in areas with heavy precipitation, steep slopes, and developed channels or drainage (Patterson, 1978). Dr. Walsh and REU students analyzed contiguous macroscopic charcoal concentrations at 1 cm intervals using 2 cm^3 of wet sediment. Samples were soaked in a 5% sodium hexametaphosphate for >24 hrs and a weak bleach solution for one hour. Samples were then sieved at 250 and 125 μm mesh screens and the residue was transferred into a gridded petri dish for counting under a stereoscope at 10 – 40X (Whitlock and Millspaugh, 1996; Whitlock and Larson, 2001). Charcoal particles were identified and counts recorded as either herbaceous or woody (for complete methods see Walsh et al., 2010).

Charcoal stratigraphy was completed for the entire lacustrine section plus an addition 10 cm of fluvial sediment and soil. The complete charcoal stratigraphy in Klickitat Lake was combined at 0-20 cm depth in KL17A and 21-103 cm in KL17B to create a complete charcoal section for the site. The combination of cores from the two adjacent locations was justified by the common marker bed found at 52 cm depth and comparable grain size stratigraphy.

2.2 Pb-210 and Cs-137 Dating of Sediment

I processed bulk sediment samples for ^{210}Pb and ^{137}Cs analyses by grinding dehydrated samples to a fine homogenous powder using mortar and pestle. Contiguous sediment samples were combined at 2-4 cm increments until total weight of the dry sediment was between 15-45 g. Samples were sent to the University of Oregon and processed in a CANBERRA low-energry germanium detector; 46.5 and 661.7 keV photopeaks were used to quantify ^{210}Pb and ^{137}Cs activity (Wheatcroft et al., 2013). The top 61 cm of sediment from Klickitat Lake and upper 100 cm from Wasson Lake were quantified for ^{137}Cs content for use as a temporal marker within the stratigraphy.

The first occurrence of detectable ^{137}Cs indicates the onset of atmospheric nuclear testing after World War II and began in November of 1952 following high-yield thermonuclear fission tests (Perkins and Thomas, 1980; Gilmore and Hemingway, 1995). A distinct ^{137}Cs peak occurred during the height of atmospheric nuclear tests in 1963, concurrent with the adoption of the Partial Nuclear Test Ban Treaty and provides a temporal marker within the lake stratigraphy (Olsson, 1986; Gilmore and Hemingway, 1995; Walker, 2005). Continual deposition of ^{137}Cs in the early 1970s can be associated with substantial activity in aboveground nuclear testing that waned near the end of the decade (Carter and Moghissi, 1977). Significant peaks from the 1987 Chernobyl Incident and destruction of the Fukushima Nuclear Power Plant by the Tohoku earthquake in Japan in 2011 were identified within the stratigraphy after the exponential decay was observed in ^{137}Cs from nuclear testing in the 1970s, and were also used as temporal markers.

Lead-210 results were variable and less precise than the age-model produced by other temporal markers, and thus the ^{210}Pb data were not used to calculate sedimentation rates.

2.3 Identification of Charcoal Horizons and Age-Depth Relationships

To compare changes in charcoal in the <250 years of stratigraphy and attempt to identify individual wildfire events, I compiled historical wildfire data from wildfire publications from the region (e.g. Impara, 1997; Zybach, 2003) that extended at least to the 18th century (Table 1). More recent wildfire activity was determined using the Oregon Department of Forestry website, (http://www.odf.state.or.us/DIVISIONS/protection/fire_protection/fires) with aid from Community Wildfire Protection Plans for North Fork (Smith River) (2004), and Lincoln County (2010).

Upon completion of radiometric isotopic dating of sediments and identification of pre- and post-atmospheric nuclear testing horizons, charcoal peaks of recorded fire events likely to have burned near and within the basin were identified in the stratigraphy. Several age-depth models were generated to justify use of charcoal horizons as stratigraphic markers, 1) an initial age-depth relationship only using ^{137}Cs temporal markers, 2) ^{137}Cs and identifiable fire events from 1951 to present, 3) all ^{137}Cs, modern and suspected historic fire events (Yaquina I in 1849, Coos Fire in 1868, and Smith River Fire in 1938). I applied the temporal markers to a constrained cubic spline (Telford, 2004). Linear sediment accumulation (SAR; cm y^{-1}) and mass accumulation rates (MAR; g cm^{-2} y^{-1}) were calculated by the slope of regression of accumulated sediment with time and by the ratio of sediment mass accumulated annually to produce the sedimentation pattern for both basins.

Significant or Proximal Fire Events				
Fire Event	**Year**	**Watershed**	**Approx. Size (km^2)**	**Depth in Core**
Yaquina I	1849	Siuslaw, Alsea, Siletz, Yaquina	1820	KL, 86 cm; WAS, 131 cm (?), 128 cm (?)
Nestucca	1853	Alsea, Siletz	1400	KL, 78 cm(?); WAS, 128 cm (?)
Yaquina II	1868	Siuslaw, Alsea, Siletz, Yaquina	1200	KL, 76 cm (?)
Coos	1868	Coos, Umpqua, Smith	500	WAS, 126 cm
Tillamook I	1933	Nehalem, Tillamook, Trask, Wilson	1250	KL, 63 cm (?)
Smith River	1938	Smith, Umpqua	160	WAS, 90 cm
Tillamook II	1939	Tillamook	845	
Tillamook III	1945	Tillamook	735	
Vincent Creek, Tioga	1951	Smith, Umpqua?	35-80	WAS, 76 cm
Tillamook IV	1951	Tillamook	130	KL, 54 cm (?)
Oxbow Ridge	1966	Smith, Siuslaw	170	KL, 30 cm; WAS, 29 cm
Silver Complex, others	1987	Rogue, Chetco, Umpqua	400+	KL, 21 cm; WAS, 29 cm

Table 1. List of significant or proximal fire events to the Klickitat and Wasson Lake watersheds that are likely found in the stratigraphy. Many additional fires are not mentioned but also likely affected charcoal concentrations, especially those prior to the 1950s and modern wildfire complexes in southwest Oregon. Modified from Zybach, 2003 with additional data from Community Wildfire Protection Plans for North Fork (2004), and Lincoln County (2010). Refer to Zybach, 2003 for complete list of major fires across the region.

2.4 Photogrammetry

I scanned aerial photos of the Klickitat and Wasson Lake watersheds at 600 DPI from the Microfilms Library at the University of Oregon to provide context for understanding 20th century land use changes and sediment chronologies. The earliest aerial photos covering the Wasson Lake drainage were taken in 1941 after the approximately 5000 ha Smith River Fire. Additional flights of the basin were completed in 1951 after the Vincent Creek Fire with regular flights afterwards in 1955, 1960, 1961, 1963, 1964, 1969, 1970, 1971, 1976, 1977, 1980, 1987, 1990, 1994, 1997, and frequently in the new millennium. The earliest available aerial photos of Klickitat Lake are from 1955 with additional flights in 1959, 1961, 1962, 1968, 1972, 1974, 1976, 1977, 1978, 1980, 1991, 1994, 2000, and into the 21st century. I georeferenced aerial photos in ArcGIS 10.5 and quantified area and length of logging roads and clear-cutting operations to compare with changes in sedimentation patterns. Changes in lake-surface area and evidence of abandoned terraces were also observed using available LiDAR data provided by Department of Oregon Geology and Mineral Industries (DOGAMI) to assess prograding delta morphology and patterns associated with watershed-scale perturbations. A master's thesis from Oregon State University by Hazards (1962) describes road building and harvesting details near Wasson Lake and provides additional information about the development of logging activity in the Wasson Creek watershed.

Chapter III

RESULTS

3.1 Core Stratigraphy

We collected cores containing a complete stratigraphic record of landslide-dammed lacustrine sediments in addition to 1-2 m of underlying soil and fluvial sediments (Figures 12 and 13). The formation of the lakes was identified in the stratigraphy based on an obvious change in grain size, color, and presence of a thin organic horizon below the first gyttja bed. The layer separating the overlying lacustrine gyttja sediment from the micaceous fluvial sediments is 2-5 cm thick, rich in organics, and overlies an abrupt irregular contact with abundant alder leaves, Douglas-fir needles, and few roots and coarse wood fragments (Figure 14). This organic layer is interpreted as the buried forest soil that was present before the lake formed.

Average grain size at both Wasson and Klickitat Lakes varies from silt to very fine sand, with the largest 10% of grains reaching medium to coarse sand in the top 10 cm of Klickitat Lake. Massive dark homogenous layers ranging from 10 to 26 cm in thickness are present in the lower half of the stratigraphy at both Wasson and Klickitat Lakes and contain dispersed coarse organics with disseminated charcoal and infrequent large (>5mm) burned wood fragments. Sediment within each lake is generally dark and composed of organic-rich gyttja with few clay-rich gyttja layers that are lighter in color. Dark layers rich in organics generally contain a hue ranging from 10YR to 2.5Y with value and chroma approaching 2.5/1, while lighter colors do not exceed a value and chroma of 5/1. Organic-rich deposits are typically darker in color with small voids and very low densities.

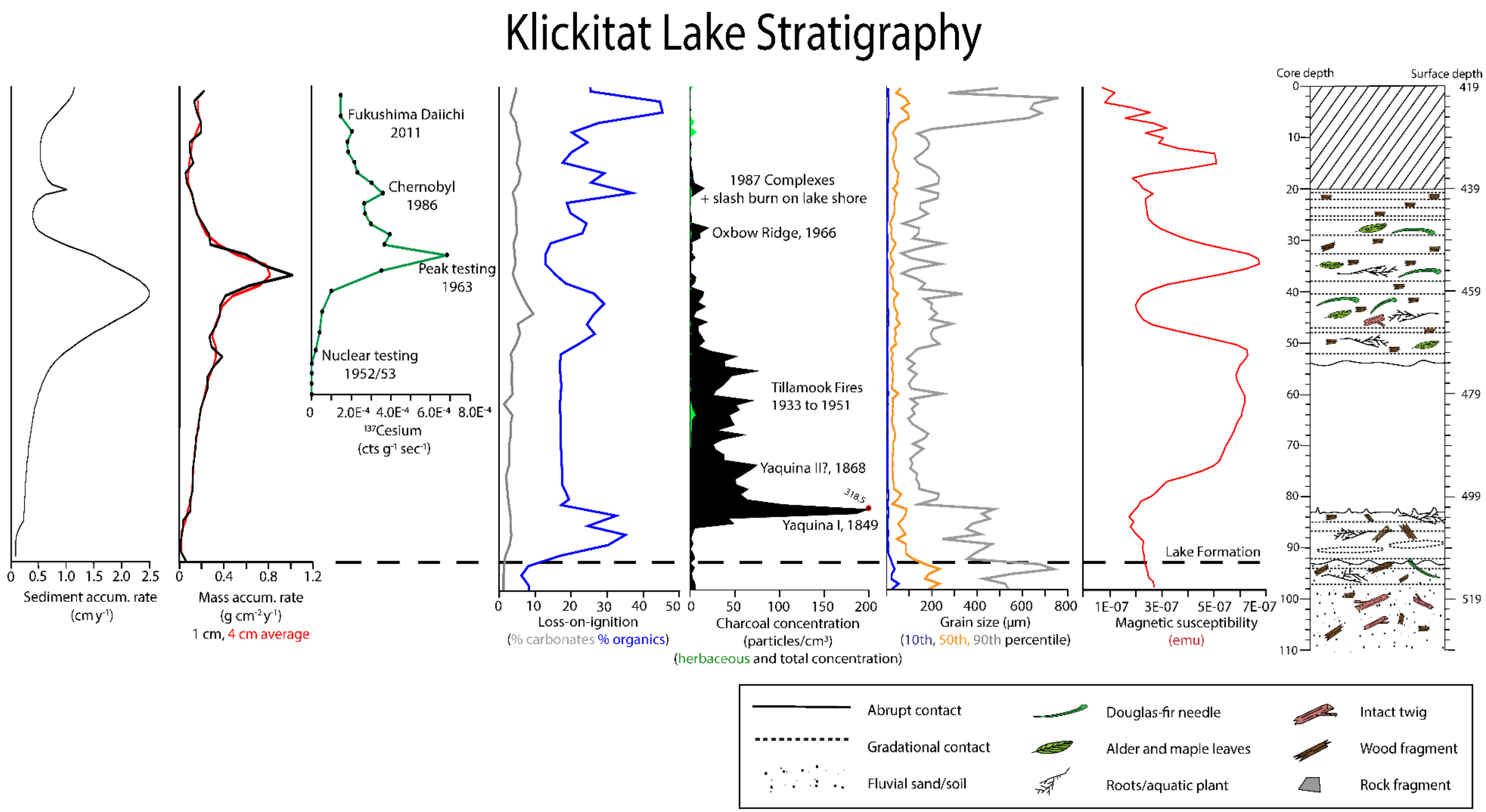

Figure 12. Compiled quantified stratigraphy with measured variables in Klickitat Lake. Parameters include; sediment accumulation rates (SAR), mass accumulation rates (MAR), ^{137}Cs radioactivity results, loss-on-ignition, charcoal concentrations, grain size analysis, and magnetic susceptibility. Lake formation is identified with dashed line at 93 cm depth.

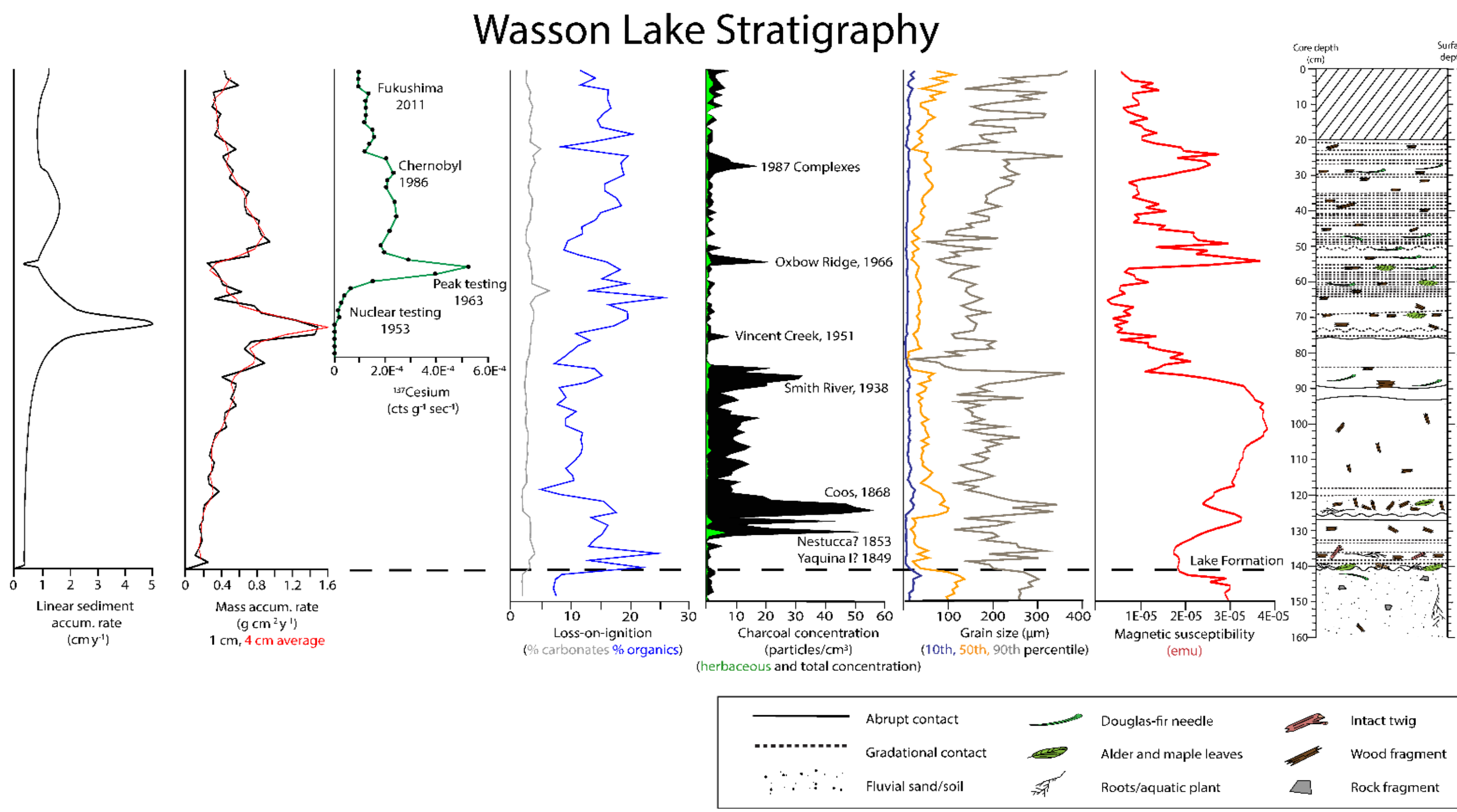

Figure 13. Compiled quantified stratigraphy with measured variables in Wasson Lake. Parameters include; sediment accumulation rates (SAR), mass accumulation rates (MAR), ^{137}Cs radioactivity results, loss-on-ignition, charcoal concentrations, grain size analysis, and magnetic susceptibility. Lake formation is identified with dashed line at 141 cm depth. Fluctuations of each parameter are similar between lakes, with Wasson Lake having more erratic behavior.

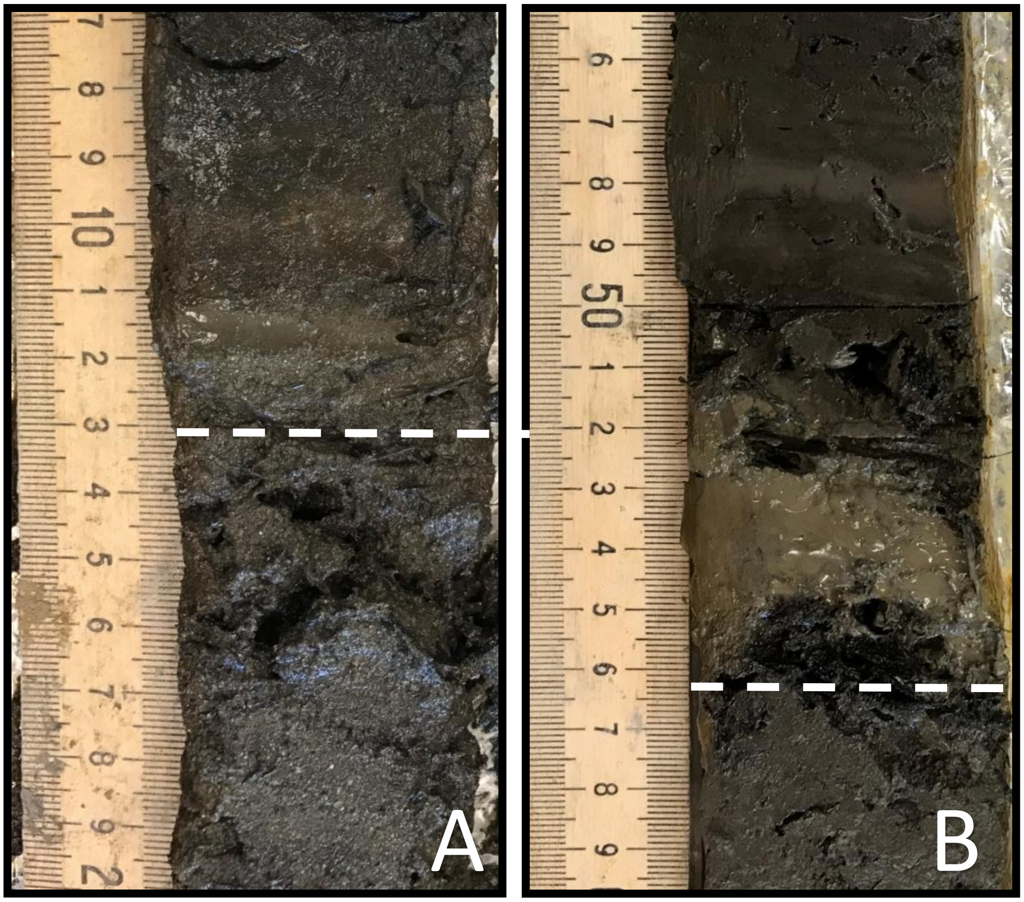

Figure 14. Interpreted onset of lake formation in Klickitat Lake (A) and Wasson Lake (B). Underlying the basal lacustrine sediments in Klickitat Lake is a sandy, organic-rich stream deposit. Underlying the lacustrine sediments in Wasson Lake is a moderately-decomposed organic horizon overlying a 40-cm thick fluvent soil.

Klickitat Lake Stratigraphy

Klickitat Lake has accumulated 93 cm of sediment since the formation of the landslide dam in AD 1751 (W. Struble and B. Black, personal communication, October 2017) (Figure 12). Below the lacustrine sediments, fluvial sands containing abundant muscovite and fragments of woody debris dominate the sediment with bedrock saprolite becoming present near 1.9 m depth.

At the stratigraphic depth interpreted as representing the formation of the lake, a decrease in average grain size from 232 µm to 44 µm is detected but distributed over several centimeters. The thin basal lacustrine deposit in Klickitat Lake grades from silt to dark grey gyttja and is overlain by a 5-cm thick olive grey horizon (5Y 3/2) with grey mottling and voids mixed with coarse organics and fine horizontal roots. This is overlain by black (5Y 2.5/1) gyttja with abundant twigs and wood fragments and coincides with the largest charcoal concentration (319 particles cm^{-3}) found at both lakes. Observable flame structures are present in the sediment 2 cm above a charcoal horizon near 83 cm depth with a rapid decrease is grain size also observed. Overlying the flame structures is a 26-cm thick very dark grey (5Y 3/1) spongy gyttja layer with high concentration of disseminated charcoal that is covered by a 2-3 cm thick marker bed composed of discernable grey (5Y 5/1) fine gyttja with very fine disseminated charcoal and organics. Overlying this sequence is a series of organic-rich deposits with poor gradational contacts that make up the remainder of the stratigraphy with a few thin laminar structures 1-3 cm in thickness visible in the uppermost 40 cm of the consolidated core. In the topmost 10 cm of the core, there is a large increase in organics and the largest grain size is observed. This material was collected separately as unconsolidated soft sediment. The stratigraphy was not preserved but is primarily composed of small fragments of woody debris.

Wasson Lake Stratigraphy

Wasson Lake is younger in age but has accumulated 141 cm of sediment since the landslide dam in AD 1819 (Figure 13) (W. Struble and B. Black, personal communication, October 2017). The formation of Wasson Lake is more obvious with a

40 cm thick fluvent soil horizon and disaggregated lithics under the first gyttja bed. Average grain size at the basal lacustrine boundary decreases from >100 µm to <25 µm with the onset of the lake with a large increase in organic content. The underlying layer interpreted as a pre-lake soil horizon contains many intact and upright aerial and shallow aquatic plant roots that disappear above the stratigraphic contact with the lake sediments. Below this, the O horizon gradationally transforms into an A horizon composed of fine sand with dispersed weathered coarse angular micaceous sandstone fragments before gradationally turning into a sandy C horizon at approximately 190 cm depth. This micaceous sand and coarse organic layer, interpreted as a fluvial deposit continues downward until a hard platy saprolite horizon at 345 cm depth from the sediment-water interface.

Sediment within Wasson Lake follows a similar pattern to that in Klickitat Lake, but sediment loading structures were not found in the stratigraphy. However, several irregular gradational and abrupt contacts are present. The largest charcoal concentration (57 particles cm^{-3}) within Wasson Lake occurs at 125 cm concurrent with a rapid rise in average grain size. Average grain size increases from ~20 µm below the charcoal layer and rises rapidly within the charcoal layer to near 100 µm. This charcoal horizon contains very coarse organics and extends for 5 cm. It transitions upward into a 27-cm thick, homogenous layer of coarse organic debris containing disseminated charcoal, abundant wood fragments, and alder leaves. Above this massive horizon, is an abrupt contact with a 4-5 cm-thick, irregular layer composed of extremely fine gyttja and fine charcoal. This layer grades from very dark grey (2.5 Y 3/1) to dark grey (5Y 4/1). Overlying an irregular abrupt contact, the sediment returns to very dark grey (2.5Y 3/1) with few coarse wood fragments with Douglas-fir needles and few fine but observable charcoal fragments. Covering the very dark layer, a gradational contact transitions to a dark grey (5Y 4/1) gyttja absent of wood fragments or charcoal. Thin laminar layers 0.25 -0.5 cm interbedded with dark, organic-rich deposits appear between 65 and 35 cm. Similar layers continue upward, but become thicker (1-2 cm) in the upper core.

Charcoal Stratigraphy

Charcoal patterns within the cores have similar concentrations at depth in the stratigraphy, with one event in Klickitat Lake briefly and substantially deviating, producing a 6 times larger peak in charcoal (Figure 12). The initial formation of the landslide-dammed lake and several centimeters of deposition contain minimal charcoal in each lake core. High charcoal deposition events occur several times in Wasson Lake between 131 and 123 cm depth with highest concentrations near 50 particles cm^{-3}. Within Klickitat Lake, several layers of charcoal are near 50 particles cm^{-3}, but a single horizon near 83 cm depth contained concentrations of 320 particles cm^{-3}, the highest concentrations recorded in this study.

High charcoal concentrations are present in the lower to middle stratigraphy and remain at both lakes until decreasing above a stratigraphic depth of 50 cm in the core from Klickitat Lake, with charcoal concentrations rapidly declining above 85 cm depth. Small isolated peaks are visible near 28 cm and 22 cm depth in the Klickitat Lake core, but decline to near zero above 20 cm.

Multiple discernible peaks are observed in the Wasson Lake stratigraphy, especially above 80 cm depth (Figure 13). An extended period of high charcoal deposition in the lower stratigraphy is similar to that in Klickitat Lake, with the last peak of sustained charcoal deposition period occurring near 85 cm depth. Charcoal concentrations decrease substantially and become close to absent at 80 cm depth, with a small peak occurring at 75 cm depth. Small amounts of background charcoal continued to flush into Wasson Lake until an observed peak at 55 cm depth. Charcoal concentrations decline again for nearly 30 cm of continuous deposition until a final distinct peak is observed near 25 cm depth.

Loss-on-Ignition and Magnetic Susceptibility

Results from the loss-on-ignition (LOI) indicate organics compose approximately 10 to >30% of the bulk density at both Klickitat and Wasson Lakes. Loss-on-ignition in Klickitat Lake is less variable while Wasson Lake fluctuates more rapidly (Refer to Figures 12 and 13). Plant organics make up the largest component of the LOI with sediment consistently having <3% carbonates. Local charcoal peaks are found to increase LOI, but other unknown variables are also at play. Unsystematic increases in organics are observed near the transition to the laminar structures in the Wasson Lake stratigraphy near 65 cm depth. In Klickitat Lake, a large increase in organics from 20% to nearly 45% is observed from 10 cm to 2 cm.

The magnetic susceptibility appears to behave inversely to the LOI, with low organic layers showing a higher magnetic susceptibility, indicating more ferrous material, and organic-rich layers showing a lower magnetic susceptibility (Figures 12 and 13). Distinct peaks in magnetic susceptibility occur in the Klickitat Lake stratigraphy near 34 cm and again at 15 cm, with high and sustained measurements from

76 – 50 cm depth. The Wasson Lake stratigraphy has a similar sustained period of high magnetic susceptibility from 130 cm to 88 cm, with individual peaks occurring at 55 cm and near 25 cm depth.

3.2 ^{137}Cs and ^{210}Pb Results

Analysis of ^{210}Pb showed mixed results at Wasson and Klickitat Lake. Significant fluctuations in radioactivity occurred in the upper 20 cm of the stratigraphy from both lakes and the ^{210}Pb radioactivity varied at depth. A clearer trend in ^{210}Pb radioactivity was observed at depth in the Klickitat Lake stratigraphy, but results from Wasson Lake were substantially more erratic. Because of these uncertainties, the ^{210}Pb results were not used for the age reconstruction in this study.

The ^{137}Cs clearly defines the onset of observable atmospheric nuclear testing and fallout in the northern hemisphere in November 1952 and the 1963 peak (Figure 15) (Gilmore and Hemingway, 1995). After the 1963 ^{137}Cs peak and the Partial Nuclear Testing Ban, exponential-like decay is observed with minor variability. Decay of the sediment begins to taper off until a discernable increase in ^{137}Cs is observed. This deviation occurs at 21 cm and 9 cm depth in the Klickitat Lake stratigraphy and at 29 cm and 7 cm in the Wasson Lake stratigraphy. Because the discernable peaks occur well after the ^{137}Cs and decay exponentially after appearing, I suggest these increases in radioactivity to be related to nuclear accidents in the northern hemisphere such as the Chernobyl disaster in April, 1986 and the 2011 Fukushima meltdown in Japan (Dibb and Rice, 1988; Ford et al., 1988; Marzo, 2014).

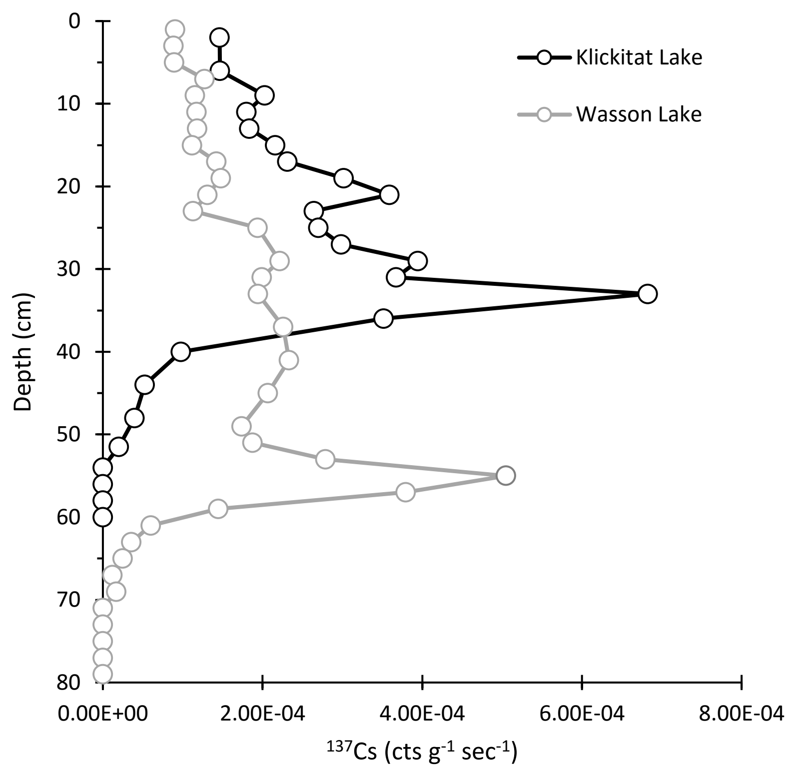

Figure 15. Results of ^{137}Cs analysis in Klickitat and Wasson Lakes. Onset and peak ^{137}Cs deposition are clearly identified with smaller peaks from the 1986 Chernobyl and 2011 Fukushima Daiichi disasters.

3.3 Generating an Age-Depth Relationship

Because radiocarbon is not practical for determining ages for these sites, the onset of each lake was based on dendrochonology of the preserved stumps that drowned during the formation of the lake (W. Struble and B. Black, personal communication, October 2017). Minimum ages of each landslide-dammed lake were confirmed at Klickitat Lake by Will Struble and team using an increment borer to identify the oldest Douglas-fir trees on the landslide deposit which began growing approximately 20 years after the damming event. The ages of the oldest trees on the Wasson Lake landslide dam were not directly applied to the age of the landslide, as they were found to have germinated after the 1880s and were identical in age to the largest trees found across sampled areas of the watershed.

I generated several cubic-spline age-depth models for Klickitat and Wasson Lakes using identifiable ^{137}Cs events as definite temporal markers (Figure 16 and 17). Recorded fire events occurring near ^{137}Cs markers were identified and charcoal layers from local fire events correlated to provide additional temporal markers in the stratigraphy.

I identified the charcoal layer from the Oxbow Ridge Fire in 1966 in the stratigraphy immediately above the 1963 ^{137}Cs maxima in both lakes. Also preserved in both lakes are the 1987 wildfire complexes which are visible in the stratigraphy concurrent with the 1986 Chernobyl ^{137}Cs peak. Near Wasson Lake, the approximately 9,000 ha Vincent Creek Fire burned approximately 5-20 km east of the watershed in 1951 and is visible in the stratigraphy immediately below the ^{137}Cs onset in 1953. The Vincent Creek Fire was a reburn of the Smith River Fire that occurred 1938, and is probably the large peak present at 90 cm depth (Figure 18). This charcoal layer was used to add additional temporal context to the stratigraphy.

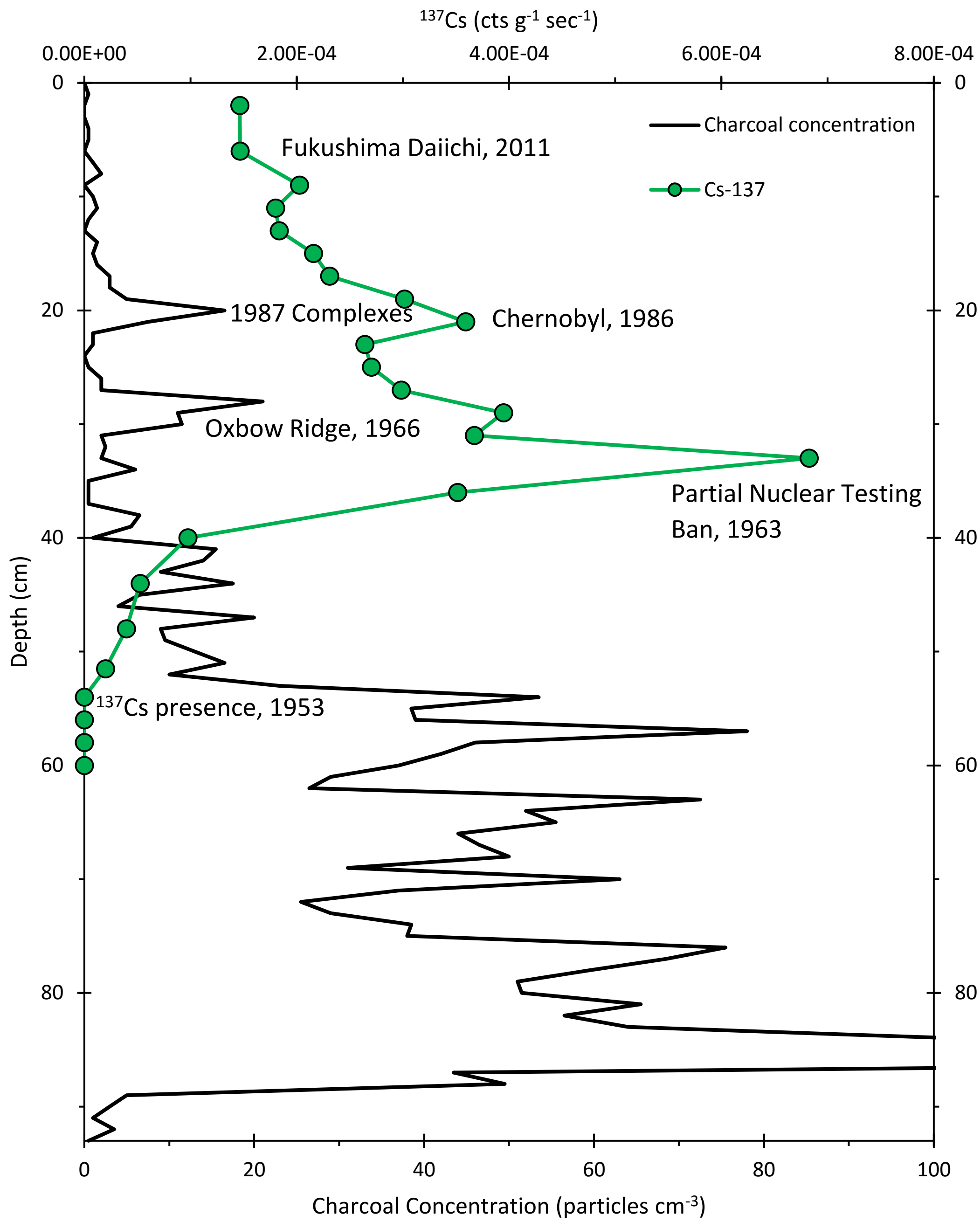

Figure 16. Comparison of ^{137}Cs and charcoal concentrations at depth in Klickitat Lake. Clear charcoal peaks from the 1966 Oxbow Ridge Fire and 1987 Complexes are identified after the 1963 ^{137}Cs apex and 1986 Chernobyl peak.

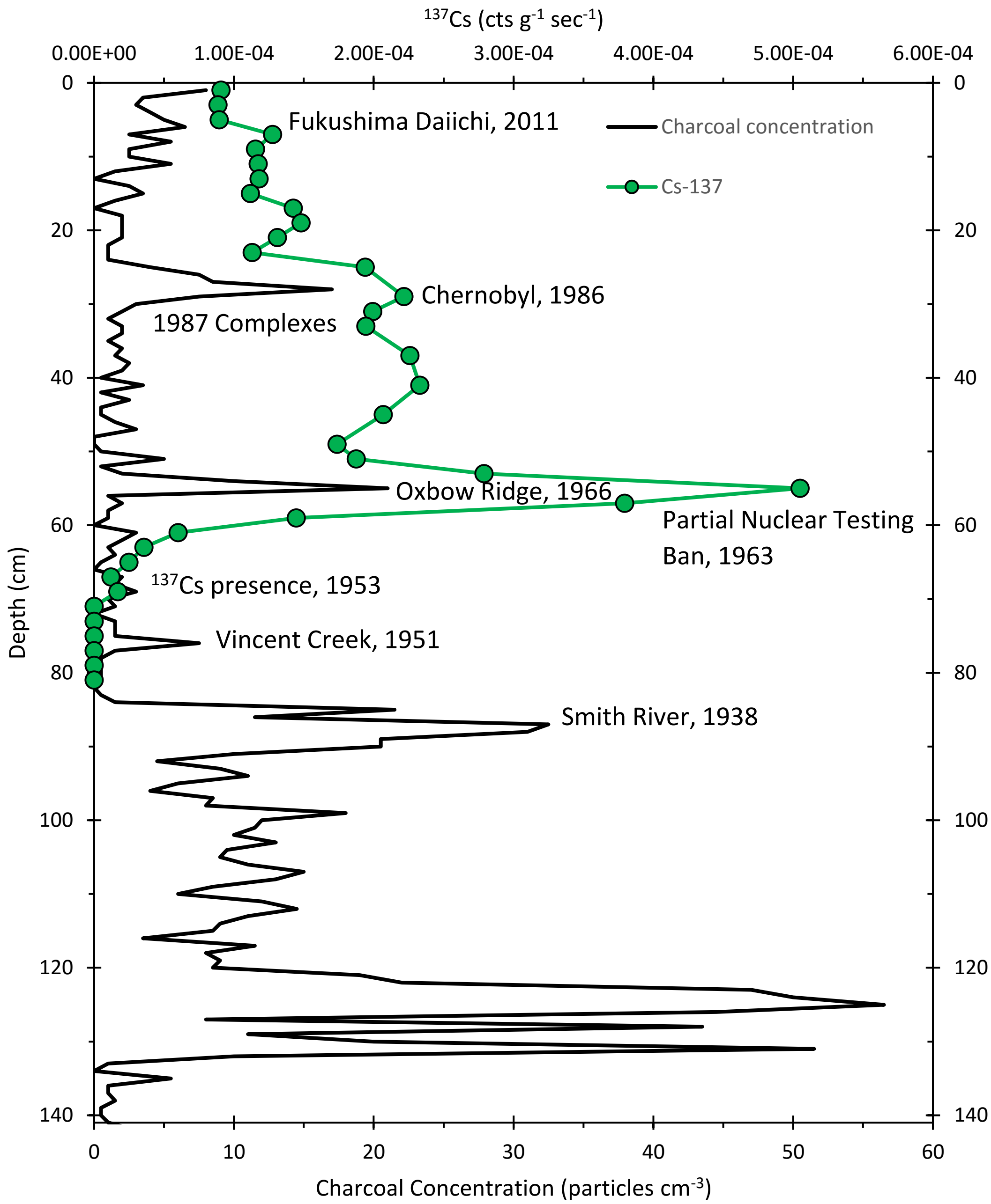

Figure 17. Comparison of the ^{137}Cs and charcoal concentrations within Wasson Lake. More distinct peaks in charcoal concentrations are present with the 1966 Oxbow Ridge Fire occurring immediately above the ^{137}Cs peak and 1987 Complexes with the Chernobyl peak. Immediately below the first presence of ^{137}Cs are the 1951 Vincent Creek and 1938 Smith River fires.

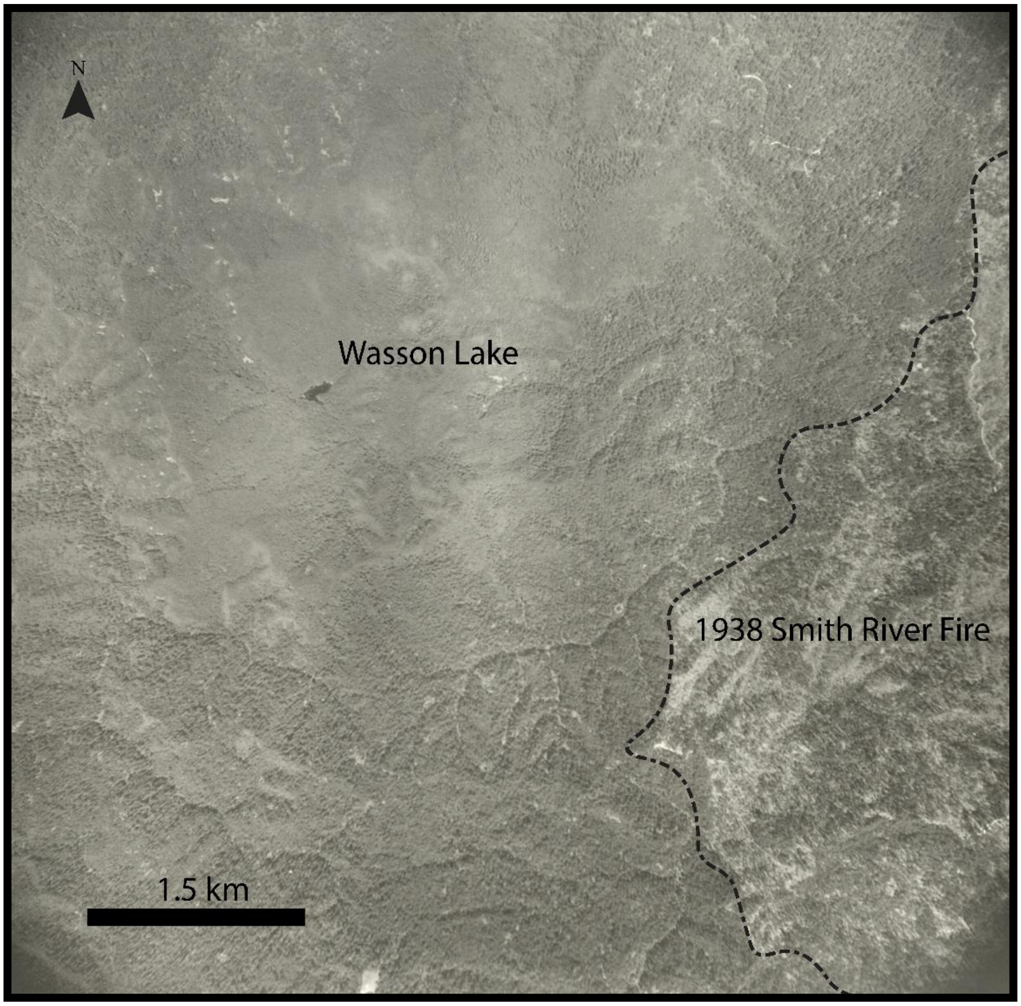

Figure 18. Earliest aerial photo of the Wasson Lake drainage with burn boundary of the 1938 Smith River Fire outlined. Boundary of the Smith River Fire is approximately 5 km from the margin of the Wasson Lake watershed. Note dense forest surrounding Wasson Lake and much of the unburned region from secondary growth after the 1868 Coos Fire.

The earliest identifiable fire event is most likely the catastrophic 1868 Coos Fire, which is recorded to have burned through the basin and is identified at 125 cm depth in the sedimentary record (Zybach, 2003). This event probably generated the largest charcoal peak early in the stratigraphy and is followed by 5 cm of high charcoal concentrations. The placement of the Coos Fire in the stratigraphy is based on the high peak charcoal concentration that is followed by high background charcoal concentrations indicative of an in-basin wildfire event (Whitlock and Millspaugh, 1996). Sampled trees in the Wasson Lake watershed all germinated after 1880, confirming the occurrence of the stand-replacing fire in 1868. The two underlying charcoal peaks at 131 cm and 128 cm are short-lived windblown events potentially from the 1849 Yaquina I Fire and 1853 Nestucca Fires, but may be from smaller, more proximal events.

Age-Depth Models

Accurate sedimentation rates of each lake are dependent on appropriate age-depth relationships. The initial age-depth models generated consisted of only ^{137}Cs and dendrochronological temporal markers (Figure 19 and 20). Identified modern fire events (post-1950) were added to the cubic-spline with only minor adjustment of the previous ^{137}Cs age-depth model, with the largest changes in the sedimentation model observed prior to the onset of ^{137}Cs deposition at Wasson Lake. The addition of the modern fire events to the model did not change sedimentation rates at Klickitat Lake.

A third scenario that incorporates suspected pre-1950 fire events to the age-depth model produced the final sedimentation age-depth relationship used for calculating sediment accumulation rates (SAR) and mass accumulation rates (MAR). In the Klickitat Lake cubic-spline, the addition of the Yaquina I wildfire in 1849 decreased estimates of early lake sedimentation rates and added minor variability to the pre-20th century sedimentation rates. In Wasson Lake, the addition of the 1938 Smith River Fire and 1868 Coos Fire minimally affected the earlier generated age-depth relationships, with the Coos Fire fitting well into the previously generated data. The close correlation of the curves generated by these three scenarios validated my use of the final age-depth model that incorporates all of the marker beds to construct MAR and SAR for the lake.

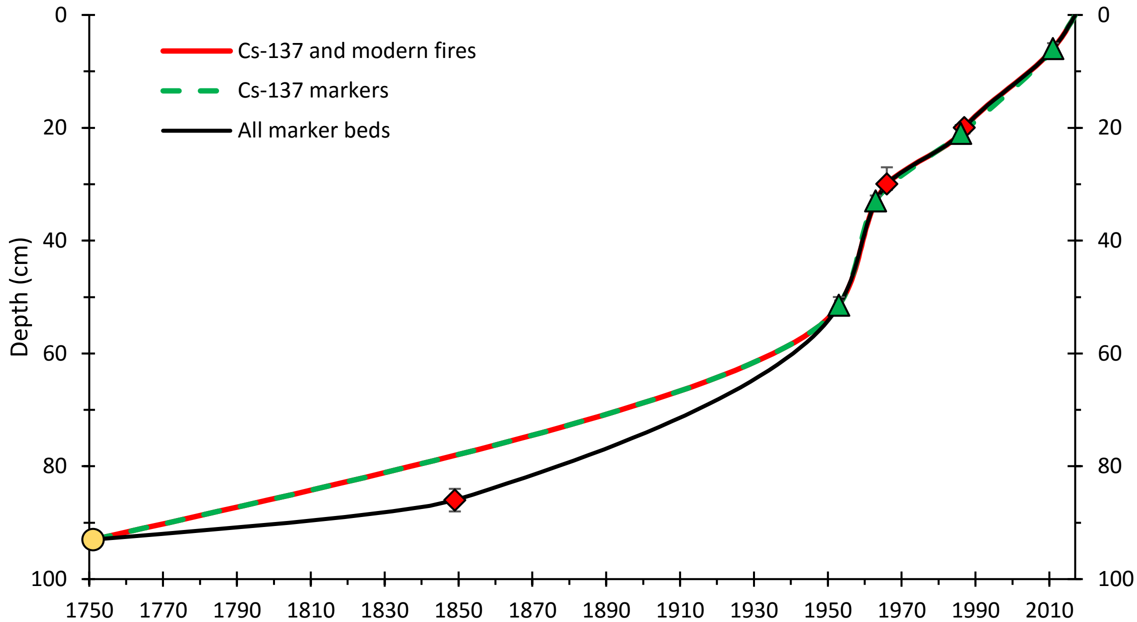

Figure 19. Age-depth scenarios compiled from ^{137}Cs (green) and identifiable wildfire events (red) in Klickitat Lake. Initial use of ^{137}Cs produces a similar curve as the addition of modern fire events to the model. Adding the Yaquina I event produces a more likely age-depth relationship.

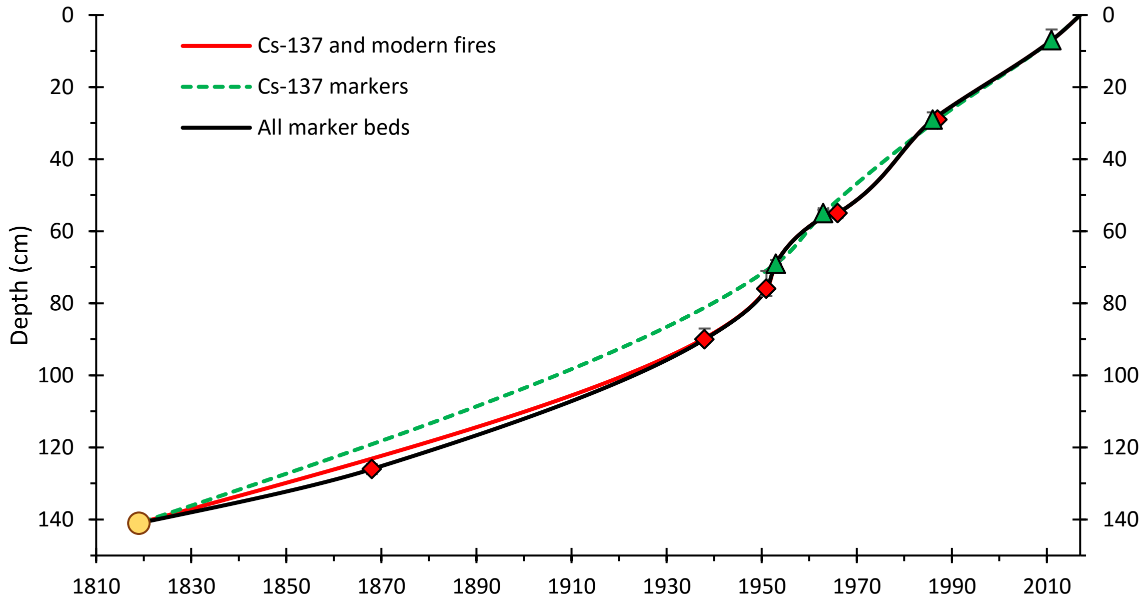

Figure 20. Age-depth relationship scenarios in Wasson Lake with age of submerged trees (yellow), ^{137}Cs markers (green) and identified wildfires (red). Initial use of only ^{137}Cs markers produces a nearly-linear trend while adding in modern and historical fire events accentuates an inflection in sedimentation rates in the mid-20th century.

3.4 Sedimentation Patterns

Linear sediment accumulation rates (SAR) provide the rate of deposition of bulk sediment load within each lake and are quantified by the thickness of material accumulated over time (cm y^{-1}). As a first-order operation, SAR are useful in understanding relative variability in sedimentation for each basin (Figures 21 and 22). Mass accumulation rates (MAR) are dependent on SAR (cm y^{-1}) and the dry density (g cm^{-3}) of individual sediment layers that are multiplied together to produce an absolute mass accumulation rate of annual sediment infilling each lake (g cm^{-2} y^{-1}) (Figures 23 and 24). Dry MAR can be directly compared between basins in the OCR to generate an understanding of available sediment load and mobility of material. Sediment and mass accumulation rates were generated from a constrained cubic spline using all ^{137}Cs markers and identified charcoal peaks as stratigraphic markers (Figures 19 and 20).

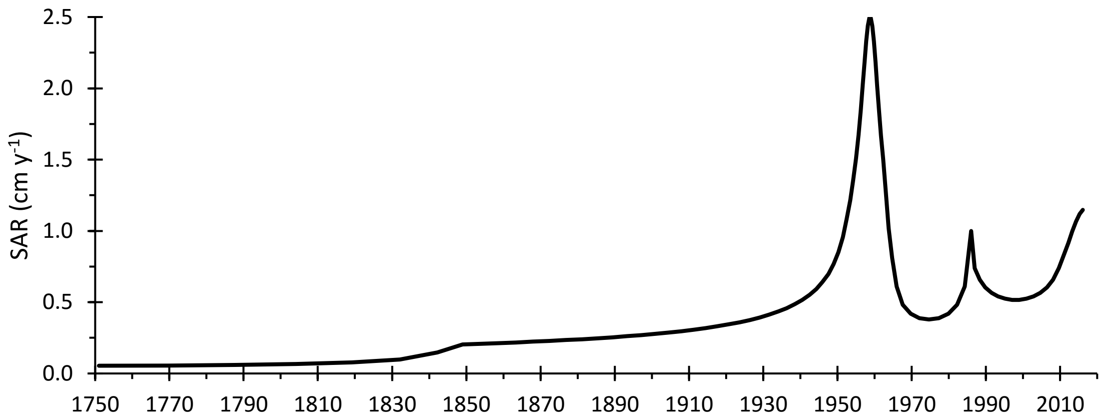

Figure 21. Linear sediment accumulation rates for Klickitat Lake using the age-depth relationship generated by using all identified marker beds. Sedimentation rates are steady prior to the 20th century before rapidly climbing in the mid-20th century and declining. Modern rates have increased and remain elevated.

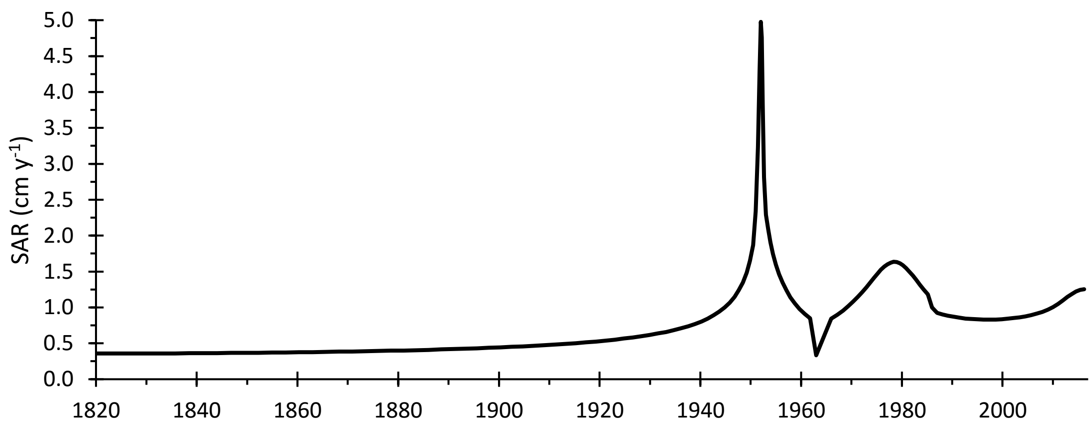

Figure 22. Linear sediment accumulation rates in Wasson Lake using the age-depth relationship generated using all identified marker beds in the stratigraphy. Sedimentation rates are low throughout the 19th century and become elevated after the 1930s. Rates peak near 1950 and decline rapidly before temporarily increasing in the 1970s. Modern linear sediment accumulation rates are elevated, similar to Klickitat Lake.

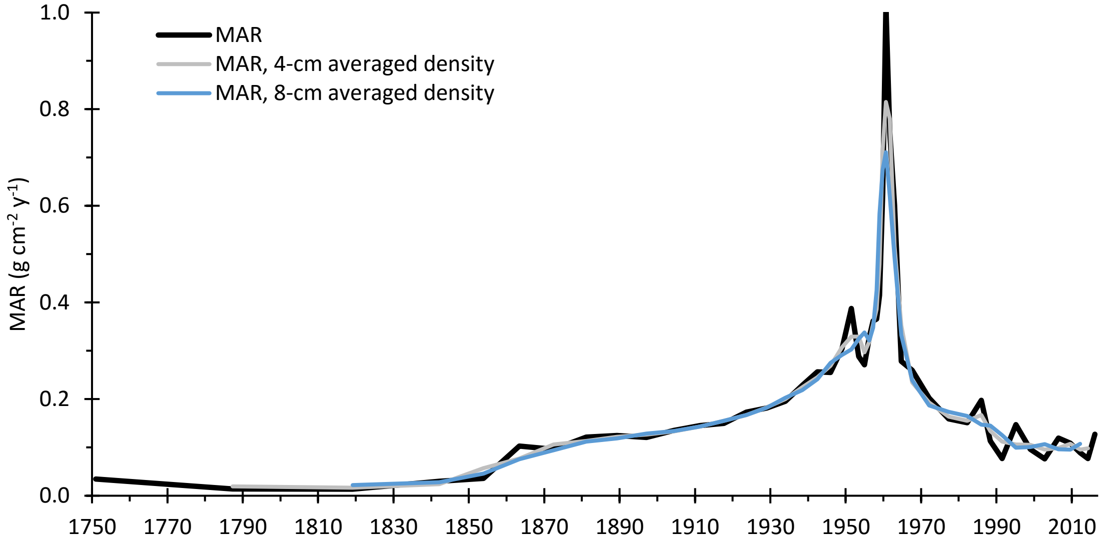

Figure 23. Klickitat Lake dry mass accumulation rates with density averaged trends. Mass accumulation is slow prior to 1850 and steadily increase into the 20th century. Rates increase rapidly approaching the 1950s and climax in 1960 before rapidly declining towards modern levels.

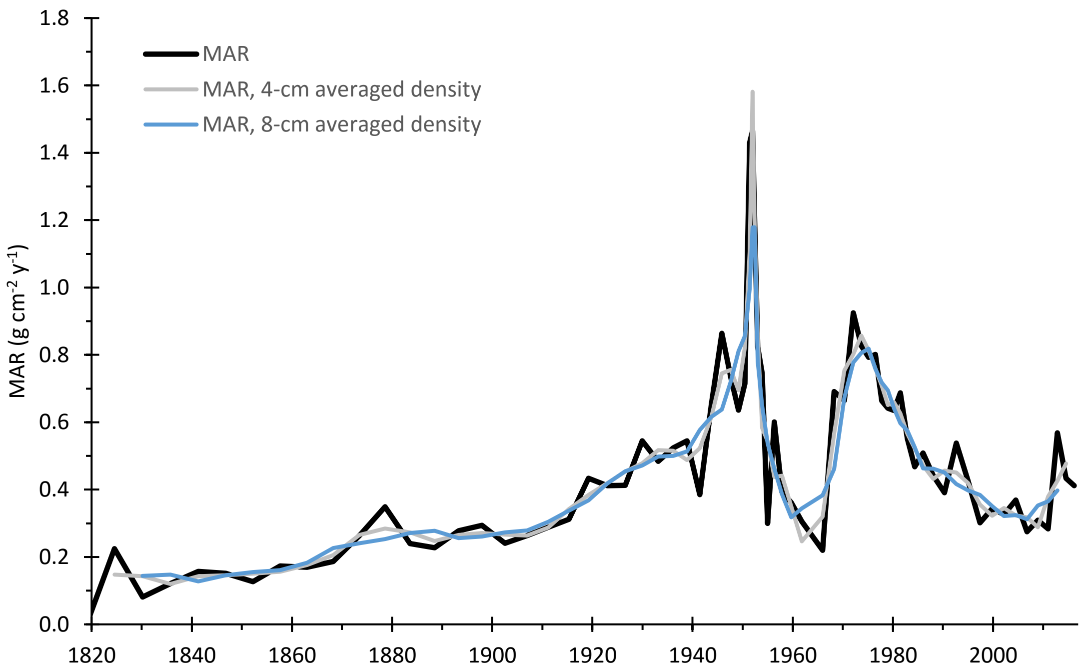

Figure 24. Wasson Lake dry mass accumulation rates with density averaged trends. Mass accumulation increases following 1870 and continue to gently climb with a rapid increase observed between 1940 and 1955. Rates decline into the 1960s but rapidly rise again near 1970 before tapering off.

Early Lake to Mid-20th Century

Early linear sediment accumulation rates (SAR) within Klickitat Lake exhibited minimal variability and were near 0.05 cm y^{-1} until quickly rising to 0.20 cm y^{-1} immediately after 1840. Rates stabilized through the end of the 19th century near 0.20 cm y^{-1} before beginning to slowly increase after 1900 and approached 0.40 cm y^{-1} by the late 1930s. Linear sediment accumulation began to increase exponentially after the 1930s before peaking in the late-1950s near 2.44 cm y^{-1}.

Mass accumulation rates (MAR) in Klickitat Lake were low throughout the 18th and early 19th century with rates between 0.01 and 0.03 g cm^{-2} y^{-1}. (Figure 25). Between the late 1850s and the 1860, a short but rapid increase in MAR increased from 0.03 to

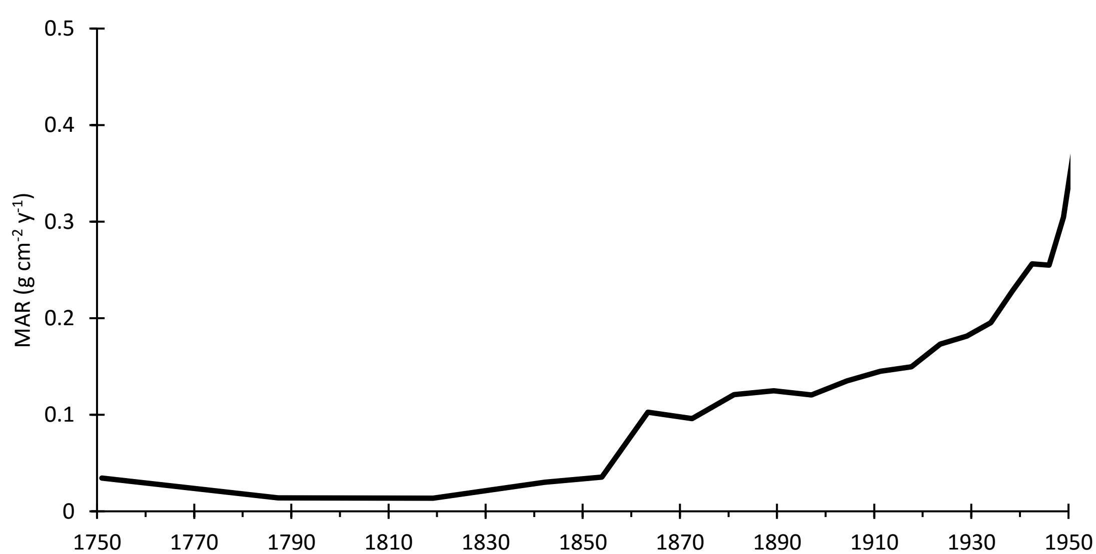

Figure 25. Early mass accumulation rates in Klickitat Lake from the formation of the lake in AD 1751 to 1950. Early rates were consistently low until a small but rapid increase after 1850. Rates continued to slowly increase until rapidly accelerating after the 1930s.

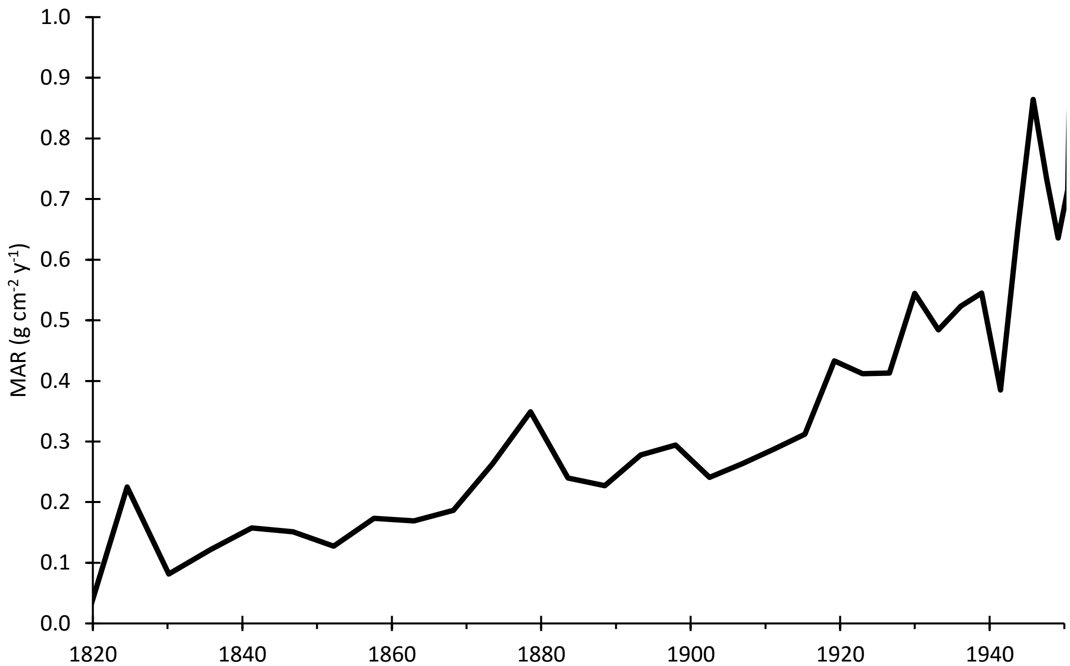

Figure 26. Early mass accumulation rates in Wasson Lake. An initial peak occurs following the formation of the lake with another small peak occurring in AD 1880. Rates continued to increase throughout the early 20th century before rapidly increasing after 1940.

0.10 g cm^{-2} y^{-1} and remained elevated. Rates slowly climbed to 0.15 g cm^{-2} y^{-1} by 1920 and continued to increase into the mid-20th century. A large increase in MAR produced a short peak of 0.39 g cm^{-2} y^{-1} in 1951 before declining and then hastily increasing to the highest observed rates near 1960.

Early sedimentation rates observed in Wasson Lake are more elevated than Klickitat Lake but follows a similar temporal pattern of increasing SAR and MAR towards the middle of the 20th century (Figure 26). In Wasson Lake, SAR began near 0.36 cm y^{-1} and slowly increased to 0.44 cm y^{-1} by 1900. Sediment accumulation remained steady until exponentially increasing after 1940 and peaking in 1952.

Mass accumulation rates in Wasson Lake slowly increased after the formation of the lake with initial MAR between 0.10 and 0.20 g cm^{-2} y^{-1}. An increase in MAR beginning after 1870 peaked at 0.35 g cm^{-2} y^{-1} before declining after 1880. Rates continued to slowly increase with several minor oscillations. Large increases were observed after 1920 with MAR peaking in 1946 at 0.87 g cm^{-2} y^{-1} and again in 1952 with the largest observed MAR of 1.47 g cm^{-2} y^{-1}.

Mid-20th Century

Substantial changes in sedimentation patterns occurred in both Klickitat and Wasson Lakes beginning in the 1940s (Figures 24 and 25). Within Klickitat Lake, SAR rose rapidly after 1940 from near 0.5 cm y^{-1} to 2.5 cm y^{-1} in the late 1950s and early 1960s before rapidly declining after 1965. By 1970, SAR had decreased to 0.38 cm y^{-1}, the lowest rates in 40 years.

The mass accumulation rate dramatically increased after 1940 in Klickitat Lake and reached an apex near 1961 of 1.02 g cm^{-2} y^{-1}. In 1940, MAR is near 0.25 g cm^{-2} y^{-1} and increases to 0.40 g cm^{-2} y^{-1} by 1950. The rate gradually declined to 0.27 g cm^{-2} y^{-1} in the mid-1950s before rapidly increasing and peaking in 1961. The rate decreased rapidly after the 1961 apex and reached 0.25 g cm^{-2} y^{-1} by the late 1960s.

The sediment accumulation rate at Wasson Lake rose sharply in the mid-20th century, increasing from 0.8 cm y^{-1} in 1940 and peaking near 1952 at 5.0 cm y^{-1} before decreasing rapidly to the lowest observed SAR of the site in 1963 of 0.33 cm y^{-1}. A small increase in SAR approached 1.60 cm y^{-1} in 1980 before declining and stabilizing.

A sharp and rapid increase in MAR occurred in Wasson Lake in the mid-20th century. After the 1920s, MAR increased continuously, reaching approximately 0.50 g cm^{-2} y^{-1} in the 1930s before a small decline to 0.38 g cm^{-2} y^{-1} in the early 1940s. MAR rose quickly to 0.86 g cm^{-2} y^{-1} in 1946 and peaked in 1951 with the largest observed MAR of 1.47 g cm^{-2} y^{-1}. After the 1951 apex, MAR dropped substantially towards pre-20th century rates with lowest observed rates of 0.22 g cm^{-2} y^{-1} in 1966. Mass accumulation very rapidly increased to 0.92 g cm^{-2} y^{-1} in 1972 before beginning a period of continual decline in MAR.

Modern Sedimentation Patterns

The uppermost portion of the stratigraphy in Klickitat Lake indicates a steady decline in both MAR and SAR since the 1970s with minor variability. Sediment accumulation rates within Klickitat Lake plummeted from 2.5 cm y^{-1} in the early 1960s to 0.38 cm y^{-1} by 1975. An isolated peak in 1986 increased SAR to near 1.00 cm y^{-1} before declining into a trough and then rising after 2005 to modern rates near 1.10 cm y^{-1}. In Klickitat Lake, MAR has fluctuated minimally since the 1970s. A small increase in 1986 increased MAR to 0.20 g cm^{-2} y^{-1} but rates have continued to stabilize near 0.10 g cm^{-2} y^{-1}.

Modern SAR within Wasson Lake have varied between 0.85 and 1.25 cm y^{-1} since 1990. After the small peak and decline in SAR in the 1980s, average modern SAR for the is near 1.00 cm y^{-1}. Modern MAR in Wasson Lake has slowly declined since the apex in 1972 with some rapid oscillations. The 1972 rise increased MAR to 0.92 g cm^{-2} y^{-1} but has continued to decline with the lowest modern rate of 0.27 g cm^{-2} y^{-1} occurring in the late 2000s. Rates have since increased with modern MAR rising to near 0.55 g cm^{-2} y^{-1} in 2012 before declining.

3.5 Anthropogenic Activity

The Klickitat and Wasson Lake watersheds both experienced periods of rapid road development and logging activity near the mid-20th century with timber harvest decreasing in the Wasson Lake basin after the early 1990s. Logging has continued in the Klickitat Lake watershed with several timber plots harvested twice since the 1960s. Both basins saw abrupt change with the rapid increase in logging activity and new forest roads installed in the late 1960's to early 1970's. Expansion of industrialized logging operations rapidly developed in the late 1960s, correlating to regional increases in clear-cutting activity of Douglas-fir across the region. Anthropogenic disturbances within the Wasson Lake watershed have been small compared to those in the Klickitat Lake watershed, which has seen continual harvest and spur road development associated with harvest of Douglas-fir timber occurring every decade since the early 1970s. Peak timber harvest varied between the two basins, but pulses of activity occurred in the mid-1970s and again in the early 1990s. The last logging occurrence in the Wasson Lake watershed occurred around 1994 with 0.11 km^2 of timber harvested, much smaller than the 0.63 km^2 harvested between 1987 and 1990.

Klickitat Lake Logging and Road Development

Significant human disturbances first occurred in the Klickitat Lake watershed during development of a single road across the landslide dam and along the eastern lakeshore by the Civilian Conservation Corps (CCC) in the mid-1930s. This isolated road was likely an access road for fire lookouts that were rapidly established across the region during the era. Beginning in 1959, a small parcel of land on the downstream toe of the Klickitat Lake landslide and outside of the studied watershed was logged by a private timber. A total of 6.4 km^2 of timber has been harvested from the 6.7 km^2 watershed with several patches logged twice since 1959 (Figures 27 and 28). Several clear-cutting operations have removed timber encircling the lake with the southern shore logged in the late 1980s and slopes of the northern shore cleared between 1978 and 1980 and again in the late 90s.

Aerial photo analysis indicate that the greatest lake level changes occurred between the 1950s and 60s, coinciding with the timing of the logging operation sometime between 1959 and 1961 and decreasing elevation of the outlet. A majority of road building occurred after this event in the late 1960s with over 14 km of roads installed by 1974. Another 5.4 km of new logging roads were installed sometime in the late 1980s. Several other small periods of logging road growth occurred as equipment roads were developed before being decommissioned after the harvest period.

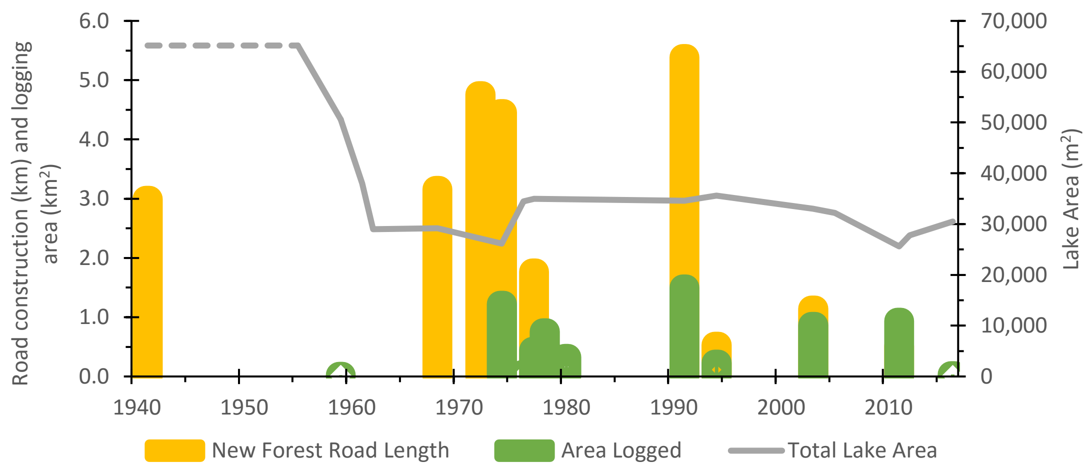

Figure 27. Length of roads developed, and timber harvested between aerial photos compared to approximate lake level dimensions. The Klickitat Lake watershed has been heavily logged since the late 1960s with several sections logged twice. Lake area substantially decreased prior to logging and roadbuilding in the immediate watershed. Road length in 1941 gathered from USGS maps (1941).

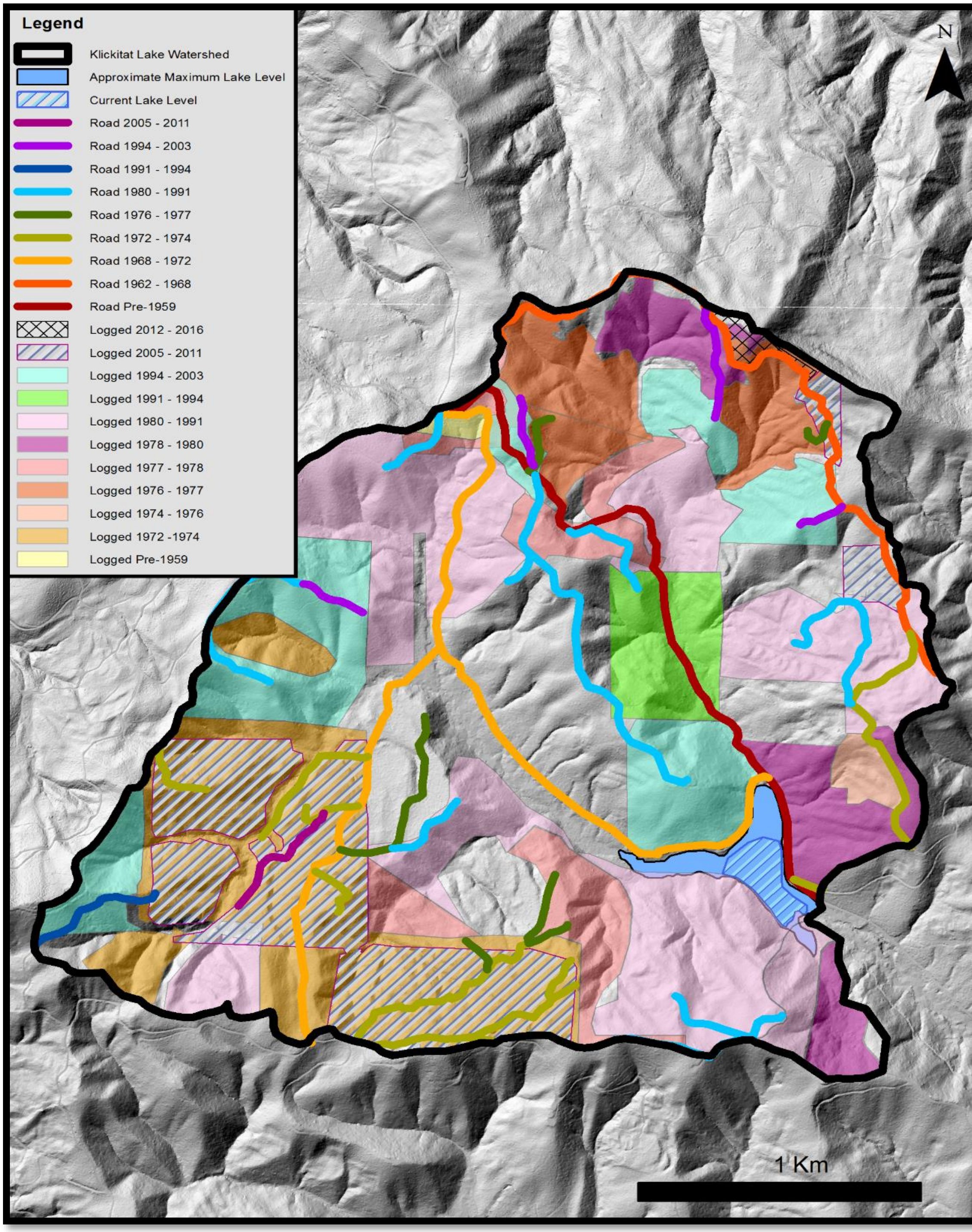

Figure 28. Classification of timber harvest and road development within the Klickitat Lake watershed. A single jeep road was present on the eastern shore prior to aerial photos in 1955.

Wasson Lake Logging and Road Development

The Wasson Lake watershed was free of logging and road building until the late 1960s when 8 km of jeep and logging roads were rapidly installed within the 3.1 km^2 watershed (Figures 29 and 30). Before this time, the Wasson Lake watershed remained untouched by industrial operations due to the long transport distance to primary roads and the less-ideal second-growth timber that germinated after the stand-killing Coos Bay Fire in 1868 (Hazard, 1962). A second phase of logging occurred between 1987 and 1990, with 0.63 km^2 logged mainly on ridges near headwater channels of the watershed. Since 1994, the watershed has been free of logging or new road construction. Wasson Creek both upstream and downstream of the lake is proposed in to be included in the future Devil's Staircase wilderness area.

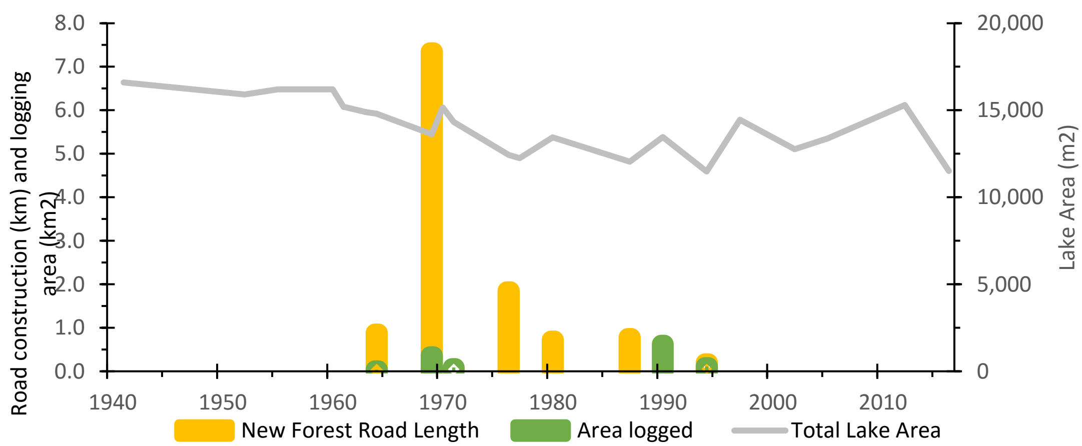

Figure 29. Length of roads and amount of timber harvested between aerial photographs compared to changes in lake level. Roads were rapidly developed in the basin after 1963 with timber harvest operations ending after 1994. Lake level has decreased minimally over the recorded period.

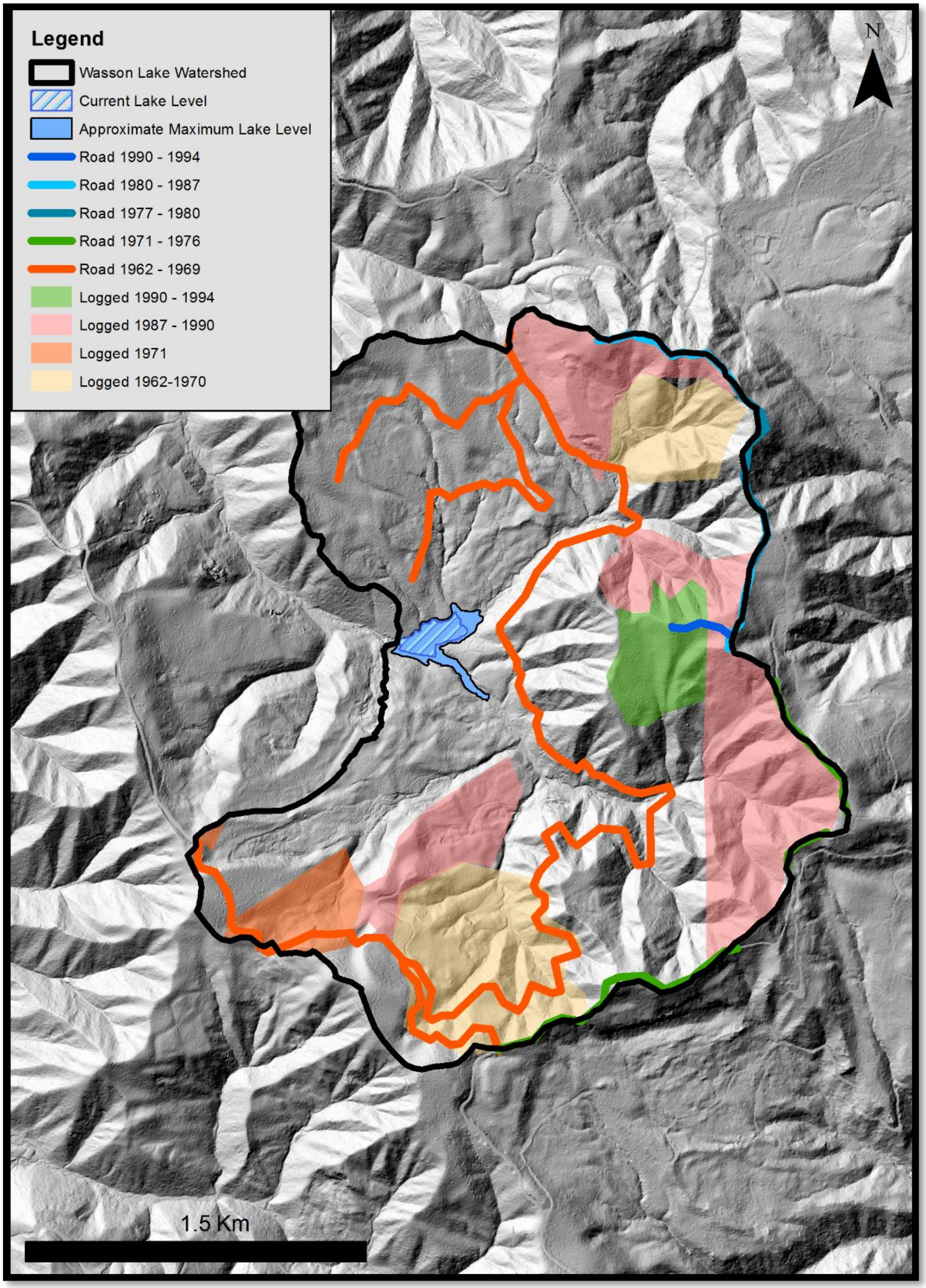

Figure 30. Classification of harvested timber stands and roads developed in the Wasson Lake watershed. No roads or other logging activity was present in the basin until the mid-1960s.

Chapter IV

DISCUSSION

Sedimentation patterns of landslide-dammed lakes in the central OCR are influenced by both natural and anthropogenic disturbances. Weather and climate fluctuations tend to have long-term effects on sedimentation rates, while proximal anthropogenic disturbances can rapidly alter organics and increase sediment availability in these small basins on short time scales. When all variables are considered, sedimentation patterns are observed in the two basins from natural- and human-derived causes.

Sedimentation in both Klickitat and Wasson Lakes have three distinct sedimentation episodes consisting of 1) formation and low sediment and mass accumulation, 2) increasing and peak sedimentation rates in the mid-20th century, and 3) lower but variable modern mass accumulation. Each lake is unique in greater-detail, but general basin-wide erosion and sediment mobilization patterns are analogous.

Early deposition within both Klickitat and Wasson Lakes suggest a transitional period in stream recovery and delta development following the formation of each landslide-dammed lake and flooding of proximal stream channels. Sedimentation and mass accumulation rates are consistently very low for this period, aside from an initial increase in MAR immediately following the formation of Wasson Lake. A rapid and continuous increase in MAR occurs in the mid-19th century following the Yaquina I Fire in 1849 at Klickitat Lake, and the Coos Fire in 1868 in the Wasson Lake watershed (Zybach, 2003). Following the stand-replacing fires and reburns in the mid-19th century, a small but distinct increase in MAR occurred.

Concurrent with a shift in precipitation and temperature patterns near the mid-1940s, rates in Klickitat and Wasson Lakes increased to their highest values in the mid-20th century. (Mantua et al, 1997). Both SAR and MAR rapidly rose to their highest levels in both lakes before peaking in the 1950s and 60s and rapidly declining. In Wasson Lake, the peak in MAR in 1951 rapidly decreased before a second peak plateaued near 1970. A general decrease in MAR and SAR has continued at Wasson Lake thereafter.

4.1 Wildfire Events

Klickitat Lake

The Yaquina I Fire in 1849 and Coos Fire of 1868 are stand-replacing fire events recorded by immigrants and Native Americans that are recorded to have burned through the lake sites (Zybach, 2003). These events were identified in the stratigraphy by the largest increase in charcoal concentration and high amounts of background charcoal following each event. Historic watershed burn boundaries and burn maps of the OCR produced by Zybach (2003) indicates both basins were subject to these large fires with the Yaquina II reburn in 1868 occurring in the Klickitat Lake region and one or more reburns likely near the end of the 19th century in the Wasson Lake drainage (Hazard, 1962). The Yaquina Fires were partially stand-replacing in the Klickitat Lake watershed, but trees well older than the fire events are still observed in the watershed today.

Outside of the Klickitat and Wasson Lake watersheds, the stand-replacing Tillamook Fires north of the study areas burned nearly 3,000 km^2 of forest in the northern OCR between 1933 and 1952 and greatly affected charcoal concentrations in the lower Klickitat Lake stratigraphy. Later evidence of the 1987 Complexes are visible near the Chernobyl-derived ^{137}Cs increase in the Klickitat Lake stratigraphy and is the last substantial change in charcoal concentrations. The 1987 charcoal peak also coincides with burning of a slash-pile or small wildfire which burned through a small clear cut on the southwestern margin of Klickitat Lake and landslide dam. Evidence of this local fire is visible on logged stumps on the southern margin of the lake and partially visible in aerial photographs.

Evidence of changes in sedimentation prior to the 20th century are sparse within Klickitat Lake aside from one distinct inflection between 1850 and 1863 (Figure 25). The small and sustained increase in both MAR and SAR are observed after the Yaquina I fire in 1849 in the Klickitat Lake watershed with MAR increasing from 0.03 g cm^{-2} y^{-1} to 0.10 g cm^{-2} y^{-1} almost 15 years after the wildfire event. No observable change is recorded after the Yaquina II reburn in 1868 until the mid-20th century. These are the only known stand-replacing fires to occur within the Klickitat Lake watershed since at least the mid-19th century and appear to have an extended influence on mass accumulation that is not substantial when compared to later fluctuations (Figure 25). May and Gresswell (2002) suggest that a rapid increase in wood within stream channels after fires potentially increased the sediment storage ability of the tributary streams, minimizing sediment deposition at the coring sites and may be partially responsible for moderating changes in sedimentation post-wildfire.

Wasson Lake

Within Wasson Lake, the ^{137}Cs onset and peak provided the initial temporal context to constrain the charcoal peaks from the 17,400 ha Oxbow Fire in 1966 and the 9,300 ha Vincent Creek Fire which burned approximately 5-20 km east of the watershed in 1951. Prior to the Vincent Creek Fire, the large peak at 90 cm depth in the stratigraphy charcoal is likely related to Smith River Fire in 1938 that burned approximately 180 km^2 of timber immediately outside the Wasson Lake watershed and was used in the age-depth model for additional temporal context in the stratigraphy. Charcoal from the record-breaking 1987 fire season is also present in the above the 1986 Chernobyl ^{137}Cs peak and also used in generating an accurate age-depth model (Figure 17). This major fire season was not from an individual burn but related to several wildfire complexes that were generated by multiple dry lightning storms that burned approximately 3,000 km^2 in southwestern Oregon and northern California with smaller burns scattered across the OCR (Zybach, 2003; Oregon Department of Forestry, 2017).

East of the Wasson Lake watershed, evidence of the 1938 Smith River Fire is clearly visible in aerial photos from 1941 with the fire burning approximately 5 km east of the basin (Figure 18). Large salvage logging operations appear to have quickly followed, moving north from Scottsburg on the Umpqua River into the burned territory.

After the stand-replacing Coos Fire in 1868 at Wasson Lake, a temporary increase in MAR is visible after the 1868 Coos Fire with maximum post-wildfire sedimentation occurring approximately 15 years after the event (Figure 26). The Coos Fire and suggested reburn by Hazard (1962) are the only known fire events to have burned in the Wasson Lake watershed since the 19th century. The nearby Smith River

Fire burned immediately outside of the watershed did not produce an increase in MAR but did produce a spike in the charcoal and organic content over a 4 cm increment. The increase in MAR associated with the Coos Fire is less sustained as the Yaquina I event at Klickitat Lake, but produces a more discernable peak following the event. Prior to the Coos Fire, MAR were near 0.20 g cm^{-2} y^{-1} in Wasson Lake but began to increase immediately following the wildfire. By 1878, MAR had peaked at 0.35 g cm^{-2} y^{-1}, a 75% increase in sedimentation. Mass accumulation rates decreased slightly after the wildfire peak, but remained faintly elevated in the following years. No observable change in sedimentation from the Coos Fire is preserved in the SAR, however, with rates remaining near 0.40 cm y^{-1}.

Stand-replacing fire events of the mid-19th century produce sustained observable changes in MAR and minor changes in SAR at both landslide-dammed lake sites. Post-wildfire MAR remains elevated throughout the pre-logging and road construction period, suggesting an increase in sediment supply that can be mobilized by the headwater channels following the fires. However, when compared to peak sedimentation rates in both lakes, these changes are minor.

4.2 Anthropogenic Disturbances

Klickitat Lake

Peak sedimentation within Klickitat Lake occurs near 1960 and coincides with a major change in lake level after a small 10 ha clear-cutting and selective logging operation began harvesting on the toe of the landslide dam between 1955 and 1959 (Figures 31 and 32). The logging operation expanded across approximately 9,000 m^2 of the lowermost toe of the landslide but was outside of the Klickitat Lake watershed. However, the modification of the toe of the landslide dam directly coincides with an approximately 1.6 m decrease in lake level and loss of approximately half of the total lake area. This human-caused decrease in lake level directly influenced peak MAR and SAR. Sediment mobilization was triggered as unvegetated lacustrine and fluvial sediments were eroded from channels and the exposed lake shore (Figure 33). These exposed sediments quickly produced a large increase in sedimentation before plants were reestablished and increased the cohesion of the recently exposed shore and channels. This lake lowering event coincides with changes in the PDO and precipitation patterns, but appears to have the largest single direct effect on sedimentation rates in the entire sediment record at Klickitat Lake.

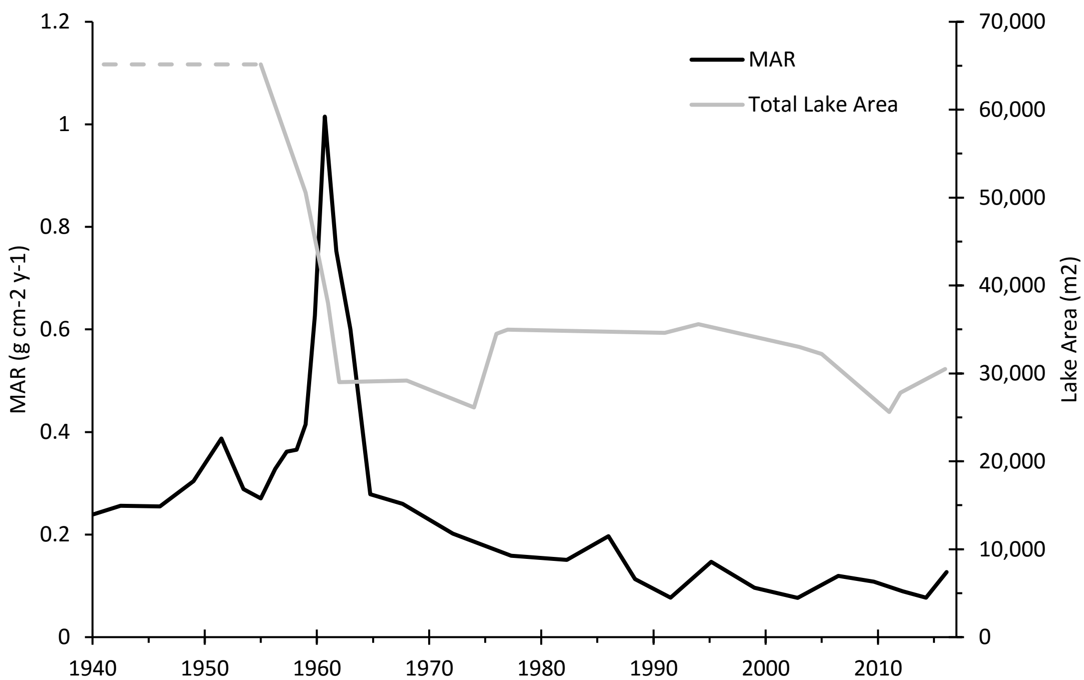

Figure 31. Mass accumulation rates in Klickitat Lake compared to changes in lake level. Peak MAR directly correlates to a 30,000+ m^2 decrease in lake levels after a small logging operation harvested the downstream toe of the landslide dam.

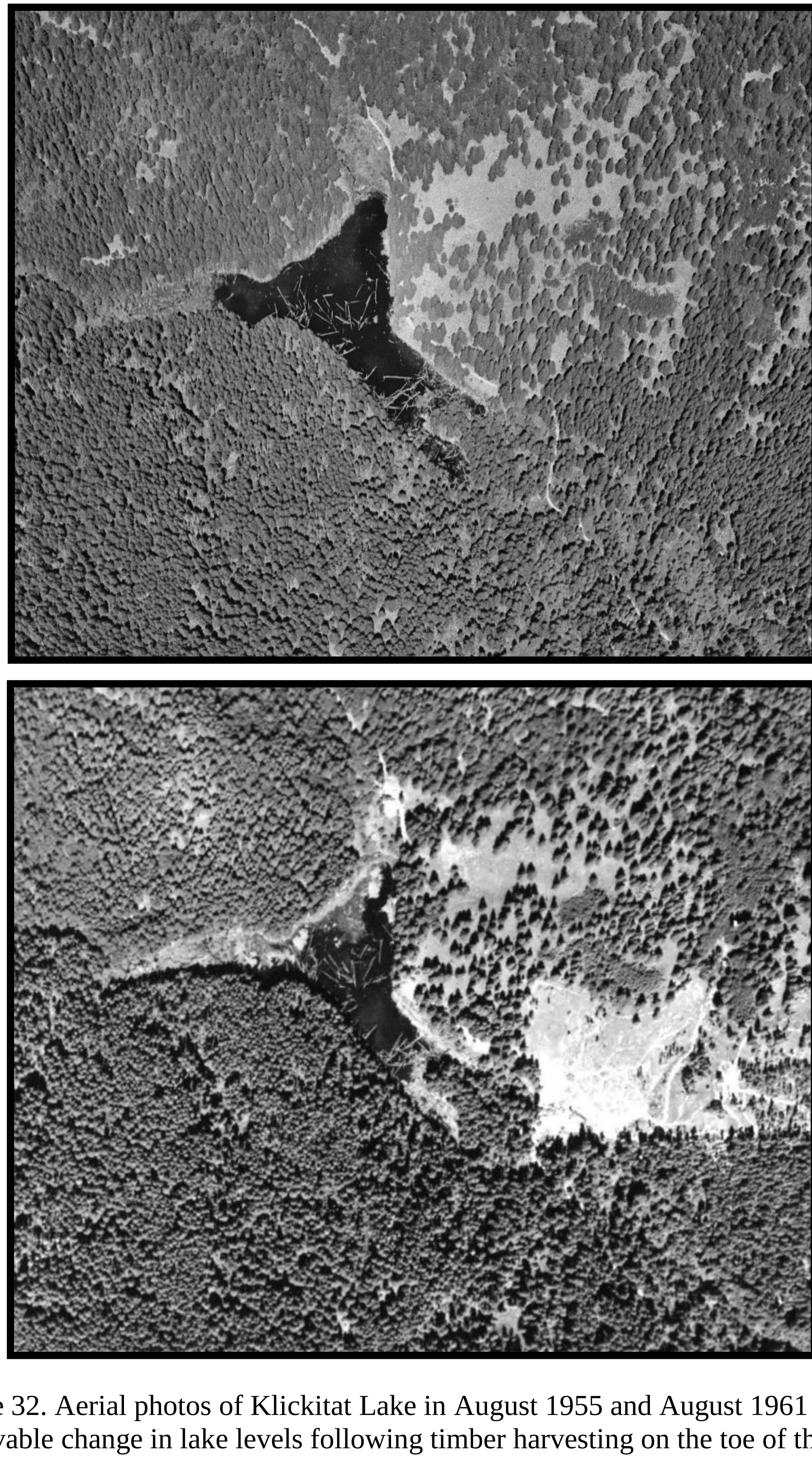

Figure 32. Aerial photos of Klickitat Lake in August 1955 and August 1961 with an observable change in lake levels following timber harvesting on the toe of the landslide dam and lake outlet.

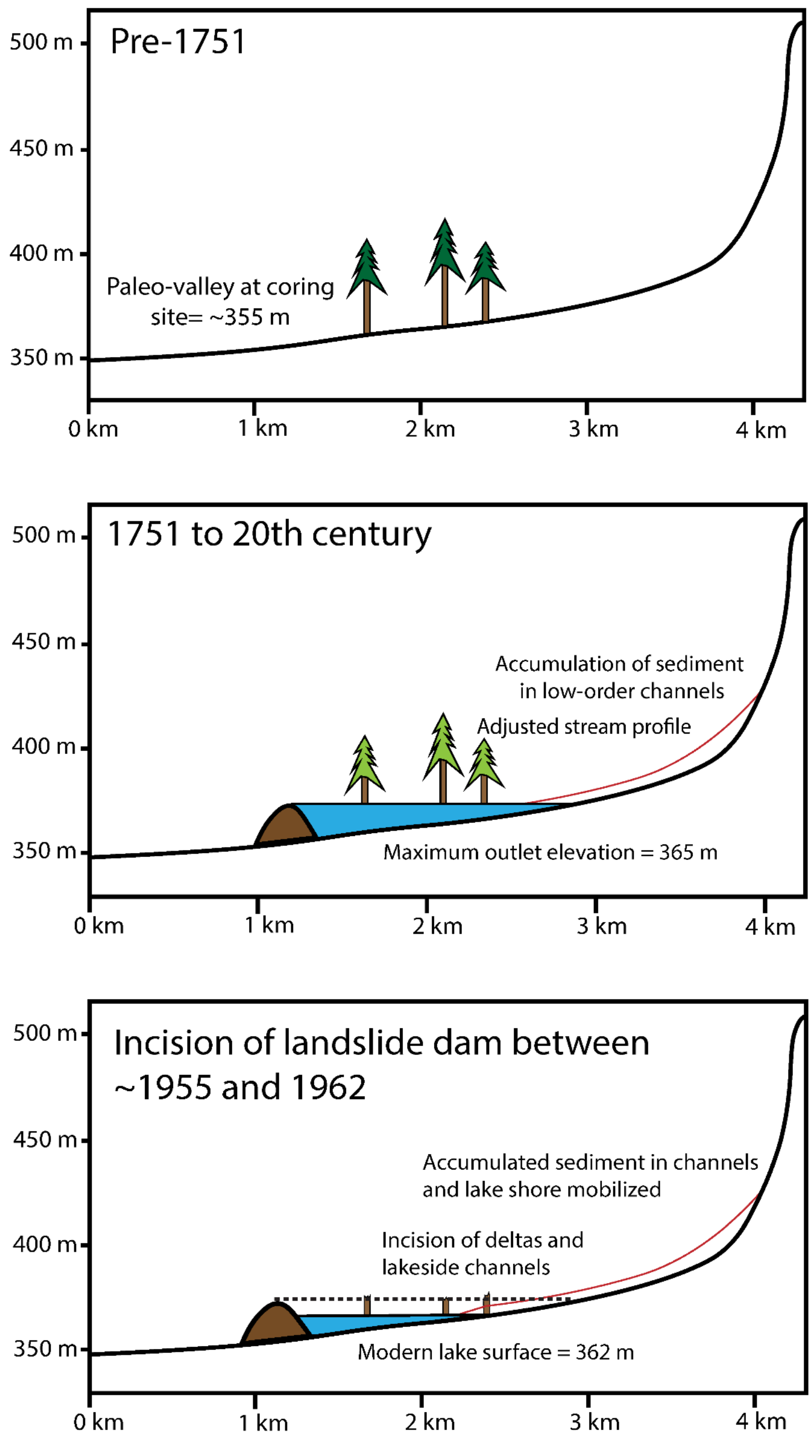

Figure 33. Schematic of effects of lake level changes on stream profiles feeding into Klickitat Lake. The largest decrease in lake level correlates to the highest mass accumulation rates observed in the entire history of Klickitat Lake.

Delayed anthropogenic effects from timber harvesting adjacent to the lake shore in the late-90s are present in the top 10 cm of the Klickitat Lake core. A sharp increase in sedimentation that was probably the result of logging on the northern shore and additional upstream sites between 1996 and 2000 increased the organic content by 25% and the largest grain size (D_{90}) by approximately 650 μm. Average grain size changed minimally, but the thick organic deposit affected sedimentation by increasing the SAR from approximately 0.5 to 1.15 cm y^{-1} with minimal changes in MAR. Similar increases in organics are observed lower in the core when the southern slope of Klickitat Lake was logged around 1987, but a change in grain size is not apparent. This is potentially due to the northern shore of the lake being a south-facing knoll with minimal channel development and thus more susceptible to dry ravel after clear-cutting, generating the large grain size associated with the high amount of organics in the upper stratigraphy. The southern boundary of the lake that was logged in the late 1980s is north-facing with prominent channels that could collect much of the coarser sediment.

This pattern of increased SAR and organics near the surface of the core at Klickitat Lake are not observed in the core from Wasson Lake, further supporting the interpretation that the logging on the shore of Klickitat Lake is the most likely cause of the increase in sedimentation at the end of the record.

Wasson Lake

Within Wasson Lake, sustained increases in mass accumulation began in the early 1950s leading to the highest peak in MAR in 1951, well-over a decade prior to roads or logging within the Wasson Lake watershed (Figure 34). Construction of over 8 km of roads within the watershed between 1963 and 1969 might have influenced the occurrence of a second period of increased MAR beginning in 1966 and peaking in 1972. Roads were not developed to the immediate lake margin, but crossed several streams that directly feed the prograding deltas in Wasson Lake. Very small amounts of road construction occurred from the 1970s to early 1990s and may have slightly increase the mass accumulation rate for short periods, but these changes are much less than the increases in 1951 and 1972. However, the largest peak in MAR occurs well before significant anthropogenic disturbance of the basin, indicating that another mechanism greatly affects sedimentation patterns.

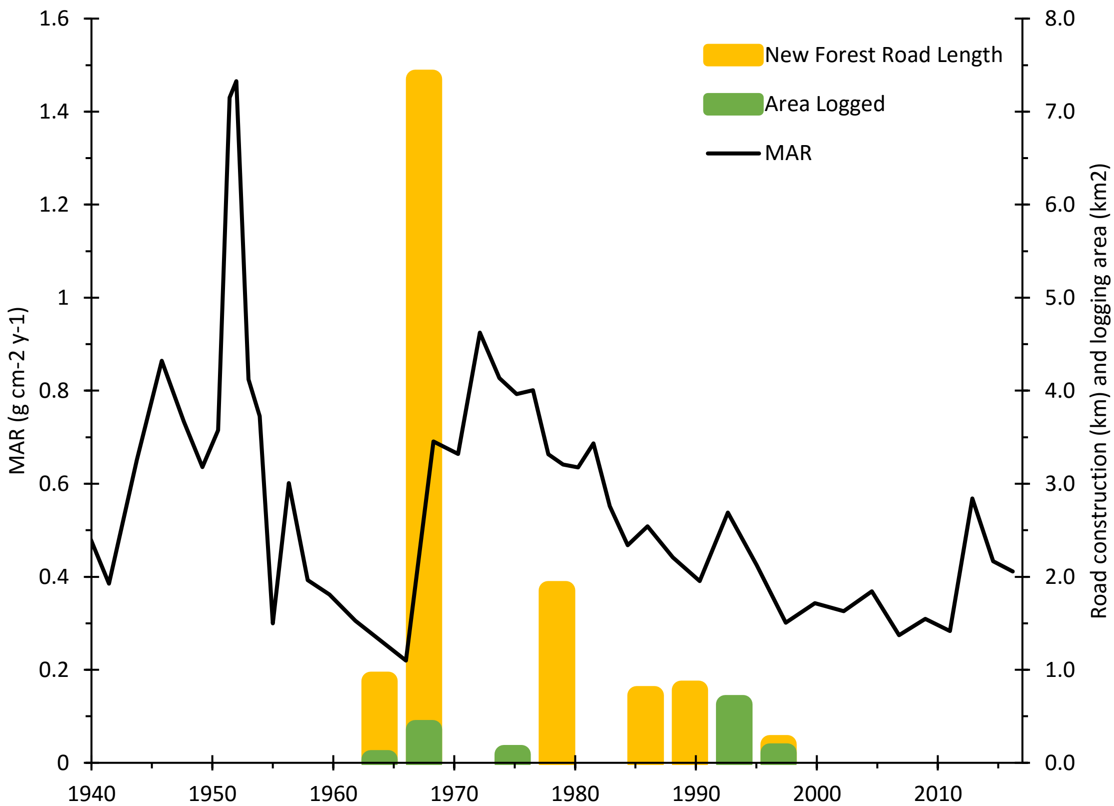

Figure 34. Mass accumulation rates of Wasson Lake compared to logging and road development. Highest MAR observed for the entire lake occurred in 1951, well before any road development in the basin. Peak construction of roads occurred between 1963 and 1969, correlating to a second increase in MAR which peaked 1972.

4.3 Climate and Precipitation Effects

Peak sedimentation rates spanning a period of 2-3 decades from 1946 to 1972 within Klickitat and Wasson Lakes coincide with an increase in precipitation and decrease in average temperatures across the entire Pacific Northwest. Peak MAR occurs near the onset of an abrupt change to the negative phase of the Pacific Decadal Oscillation (PDO) that tends to lead to cool, wet conditions in the Pacific Northwest (Mantua et al., 1997) (Figures 35 and 36). The PDO is a statistical index of changes in sea surface temperatures and atmospheric pressures in the northern Pacific Ocean that often correspond with fluctuating decadal-scale terrestrial climates in western North America and elsewhere (Mantua and Hare, 2002). Cool-wet or warm-dry climatic conditions lasting several decades have been associated with particular phases of the PDO.

When compared to the PDO index, a clear increase in MAR and SAR in both lakes is observed coinciding with the shift towards the cool-wet regime from 1946 to 1976 (Figures 35a and 36a). This transition in the mid-1940s is the most dramatic shift in the PDO since ocean temperature records became readily available. The MAR gradually increased prior to the shift toward the cool-wet period, but the dominant peak in sedimentation in the 250-year lake record coincides with this transition in PDO.

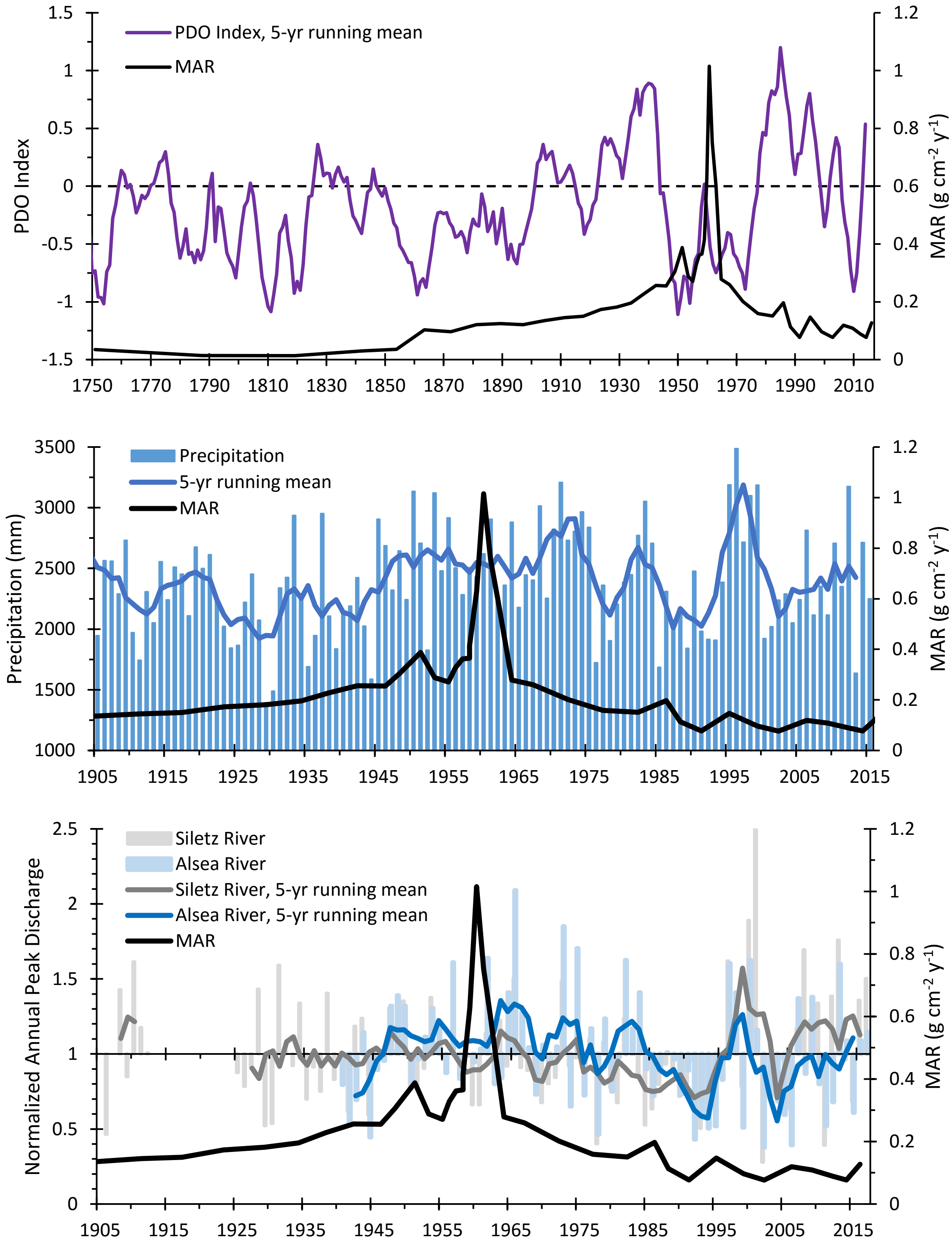

Figure 35. Mass accumulation rates of Klickitat Lake vs a) Pacific Decadal Oscillation (modified from Deser et al., 2012), b) annual precipitation, and c) peak annual discharge events.

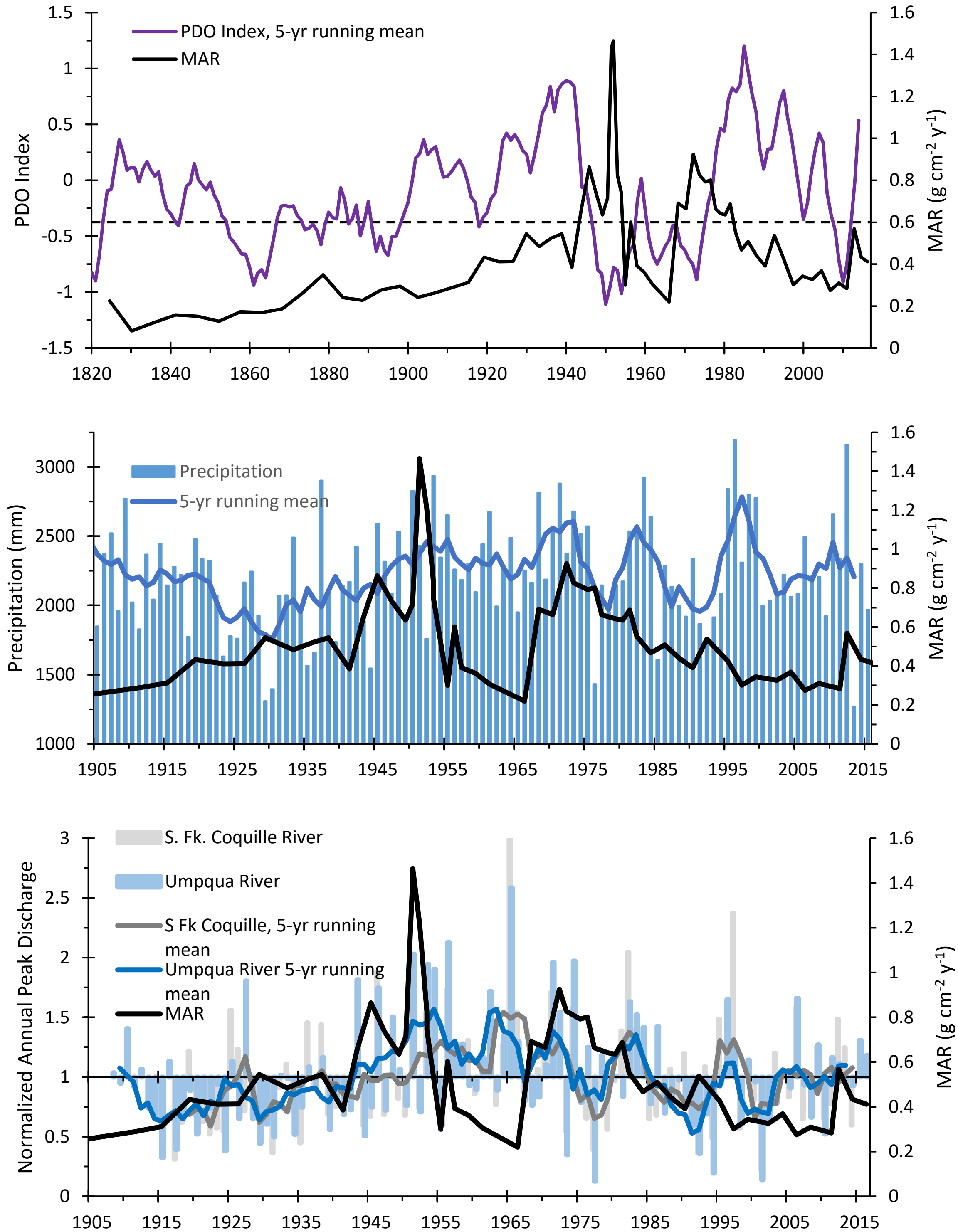

Figure 36. Mass accumulation rates of Wasson Lake vs a) Pacific Decadal Oscillation (modified from Deser et al., 2012), b) annual precipitation, and c) peak annual discharge events.

Sustained climatic periods associated with the PDO could potentially affect wildfire abundance and mobilization of shallow and deep-seated landslides in the Pacific Northwest (Mantua et al, 1997; Hessl et al., 2004; Mackey, 2009). Systematic tracking of earthflow surfaces by Mackey (2009) found an increase in velocity of earthflow surfaces concurrent with the cool-wet phase in the PDO in the Eel River catchment in northern California. Because debris flows and episodic mass-wasting events are the primary drivers of sediment delivery to channels, it is not unreasonable to associate this change in regional climate and landslide mobilization with a potential influence on sedimentation patterns in Klickitat and Wasson Lakes. These findings are further supported by results from Richardson (2017) at Loon Lake, 20 km south of Wasson Lake. Results from Loon Lake show increased sediment production and mobilization to sediment repositories in the mid-20th century related to climate and precipitation regime. Using varved sediments spanning the last 75 years, Richardson (2017) identified 1946 as the highest modern MAR, which coincides with the initial sharp rise in MAR at both Wasson and Klickitat Lakes that led up to the peak MAR at Wasson Lake and the initial peak in sedimentation at Klickitat Lake less than 5 years later. These perturbations during the cool-wet phase of the PDO in multiple studies within the region strongly suggest that precipitation, temperature, or peak discharge events may individually or collectively affect erosion and sedimentation patterns in the two small watersheds in this study.

Klickitat Lake Precipitation and Climatic Patterns

Sedimentation patterns in Klickitat Lake were influenced by the incision of the dam and lowering of the lake level around 1960, but an earlier climatic signal is observed with SAR and MAR beginning to increase dramatically after the 1930s. Annual precipitation increased after 1945 and was elevated until decreasing after 1975 (Figure 35b). A sustained period of particularly frequent high peak annual discharges on the nearby Alsea River also occurs from 1945-1975, although the pattern is not as obvious in the Siletz River watershed north of the site (Figure 35c). Elevated discharge events returned briefly in the early 1980s before substantially declining through the early1990s.

An increase in annual precipitation beginning after 1945 directly correlates with the initial increase and small peak in MAR in 1951. Lake levels in Klickitat were not yet altered at this point, indicating that the increase in MAR was most likely a product of climatic changes during the period. After lake levels stabilized in the 1970s, precipitation patterns were still elevated but do not appear to alter sedimentation patterns, especially in the wet years of the late 1960s, 1970s, and mid-1990s. A small increase in MAR is observed near 1995, but is not as substantial as the increase in the early 1950s.

No obvious direct correlation between peak discharge events and sedimentation are observed in Klickitat Lake (Figure 35c). The largest recorded flood events have minimal to no impact on MAR, with the large flood in December, 1964 occurring several years after the greatest pulse of sediment was delivered to the basin. Again, lake levels directly affected sediment mobilization for this period, but the lack of fluctuating

MAR with flood events suggests that sedimentation in the Klickitat Lake watershed is not substantially affected by the heavy rainfall patterns that produce floods in larger watersheds.

Wasson Lake Precipitation and Climatic Patterns

Sedimentation patterns in Wasson Lake are more variable than Klickitat Lake, but follow similar trends of low initial MAR, a rapid increase in MAR from 1940 to 1972, and variable but decreasing modern rates. Similar to the region of the Klickitat Lake watershed, annual precipitation near Wasson Lake increased after the 1920s coincident with the rapid increase in sedimentation after 1940 (Figure 36b). Peak sediment deposition occurred in 1951 during a high precipitation period, after which MAR decreased rapidly into the late 1950s and early 1960s. A rapid increase in MAR in the late 1960s correlates with an increase in annual precipitation but begins to decline into the 1970s. Several periods of elevated precipitation occur near 1980 and 1995, but do not have a direct influence on sedimentation rates.

Peak discharge events appear to have a partial role in increased MAR and SAR in the Wasson Lake drainage, especially when coupled with high annual precipitation (Figure 36c). On the Umpqua River and South Fork of the Coquille River, high peak discharge events occur annually to biennially starting in the mid-1940s, and this high frequency continues until the mid-1950s. However, isolated flood events (e.g. 1965 and 1996) do not appear to immediately affect sedimentation. The sustained period of high precipitation and peak annual discharges between 1943 and the early 1950s that coincides with the substantial intensification in the MAR, indicates that the coupled high peak discharges and precipitation are most likely the dominant factors affecting sedimentation mobilization in the Wasson Lake watershed. This observed increase in sediment deposition in the mid-20th century occurs over a decade prior to any substantial anthropogenic disturbances, which further supports the interpretation of climate as the major driving force of erosion and sedimentation in this watershed.

A second pulse of increased sedimentation occurred in the late 1960s to early 1970s, but does not show a strong link to any single triggering factor. This pulse follows the large 1964 flood, which is the largest modern flood event recorded in the basin, although annual precipitation is not exceptionally high when compared to adjacent years (Figure 36b). The pulse in MAR coincides with a moderate increase in precipitation as well as the onset of road development and initial timber harvest in the Wasson Lake watershed, which could have contributed to the mobilization of sediment to the channels and exacerbated the second peak in MAR. This pulse occurred in the latter stage of the sustained period of negative PDO and generally higher precipitation and river discharges.

Similar to Klickitat Lake, the transition into the cool-wet period of the PDO in the mid-1940s directly correlates with peak MAR and SAR in Wasson Lake (Figure 36a). Also similar to Klickitat Lake, previous shorter-term fluctuations in the PDO do not appear to have any effect on earlier sedimentation rates. The ideal fit of Wasson Lake sedimentation patterns with the negative phase of the PDO cycle suggests that the climatic conditions associated with the PDO play a role, perhaps influencing the multiple variables (e.g. precipitation, peak discharge, temperatures) that appear to be necessary to produce the high MAR and SAR observed in the mid-20th century.

Sedimentation in Other Landslide-Dammed Lakes in the Oregon Coast Range

Results from MAR in Wasson and Klickitat Lake are comparable with large landslide-dammed lakes in the OCR. Recent results from Loon Lake, 20 km south of Wasson Lake (Richardson et al., 2017) show that long-term mass accumulation patterns over the last 1500 years averaged 0.41 – 0.46 g cm^{-2} y^{-1}, while the modern MAR from 1979-2012 averaged 0.58 (0.48-0.70) g cm^{-2} y^{-1}. The rate from 1979-2012 is similar to that of Wasson Lake (0.43 g cm^{-2} y^{-1}) but is significantly higher than the MAR in Klickitat Lake for the same period (0.12 g cm^{-2} y^{-1}). Chronologic reconstruction from varves present in the upper stratigraphy of Loon Lake indicate that the highest MAR in the basin occurred in 1946, simultaneous with the large increase in Wasson Lake during the onset of the cool-wet phase associated with the PDO (Richardson, 2017). During the entire cool-wet period of the PDO from 1939 to 1978, Loon Lake generated a MAR of 0.79 g cm^{-2} y^{-1}, and Wasson Lake had a similar MAR of 0.71 g cm^{-2} y^{-1}; however MAR in Klickitat only increased to 0.39 g cm^{-2} y^{-1}. Results from Little Lake, a dissected landslide-dammed lake in the central OCR, showed MAR ranging from 0.04 to 0.19 g v cm^{-2} y^{-1}, similar to the lower MAR rates observed in Klickitat Lake outside of the mid-20th century peak (Long et al., 1998). Outside of the Tyee Formation, MAR calculated from ^{210}Pb at Devil's Lake on the central Oregon Coast produced a sedimentation rate of 0.14 g cm^{-2} y^{-1} for the last century (Eilers et al., 1996).

Comparable results from lakes in the OCR are promising, with the southern region having higher MAR at both Loon Lake and Wasson Lake. Little Lake is located between Klickitat and Wasson Lakes in the central Tyee Formation and has similar sedimentation rates to Klickitat Lake in the northern area of the formation (0.04 – 0.19 g cm^{-2} y^{-1}). Rates of sedimentation are expected to be higher at Little Lake when comparing the spatial distribution of Wasson and Klickitat Lakes in the Tyee Formation, but the substantially older Triangle and Little Lakes (approximately 50,000 y) have partially filled with sediment and decreased the gradient of channels, potentially affecting recent sedimentation rates (Worona and Whitlock, 1995). Considering Devil's Lake location outside of the Tyee Formation but comparable MAR to Little Lake and Klickitat Lake, Loon and Wasson Lakes could be outliers. However, more sediment studies of small lake sites would be beneficial in understanding the temporal and spatial distribution of sediment mobilization in OCR.

4.4 Formation and Stability of Landslide-Dams

Only three landslide-dammed lakes have formed in the OCR during recorded history: Ayers Lake (December 6th, 1975), Gould (Elk) Lake (approx. 1894) and the temporary Camp Creek landslide-dam in winter 1955-56, which failed within a month of its formation (Lane, 1987; Roering et al., 2005, Zybach, 2003). The number of failed landslide dams is unknown but is expected to exceed that of stable landslide dam sites. More examples are required to understand the pattern of landslide-dam stability in the OCR.

The most obvious characteristic of all small landslide-dammed lakes visited in the OCR region is the presence of large log jams located at the outlet of the lakes. This agglomerate of wood can completely mask the presence of flowing water but suggests that large woody debris may play a role in the stability and reduced incision of the landslide dams (Figure 37). Aerial photos from the 1940s and 1950s of Klickitat and

Wasson Lakes indicate that many of the floating or partially buried logs against the lake outlet have moved very little and add to the stability of the landslide-dammed lakes.

Figure 37. Abundant floating woody debris in Burchard Lake (OCR) and Wasson Lake. Initial landslide-dam formation and first overflow incision event likely moderated by floating debris acting as log jams near the narrow outlets, minimizing initial incision during first-fill and peak precipitation events.

Salmon were personally observed spawning in Yellow Lake and Gould Lake in the southern Tyee Formation, demonstrating that the landslide dam and log mats are not impassable for anadromous fish. Within the landslide deposits, buried old-growth Douglas-fir and cedar trees can form barriers in stream channels and could be a component in the stability of the initial lake formation, especially in narrow channels. The importance of this factor should be studied in greater depth in the future when assessing landslide-dam stability indices at other landslide-dammed lakes across Western Oregon.

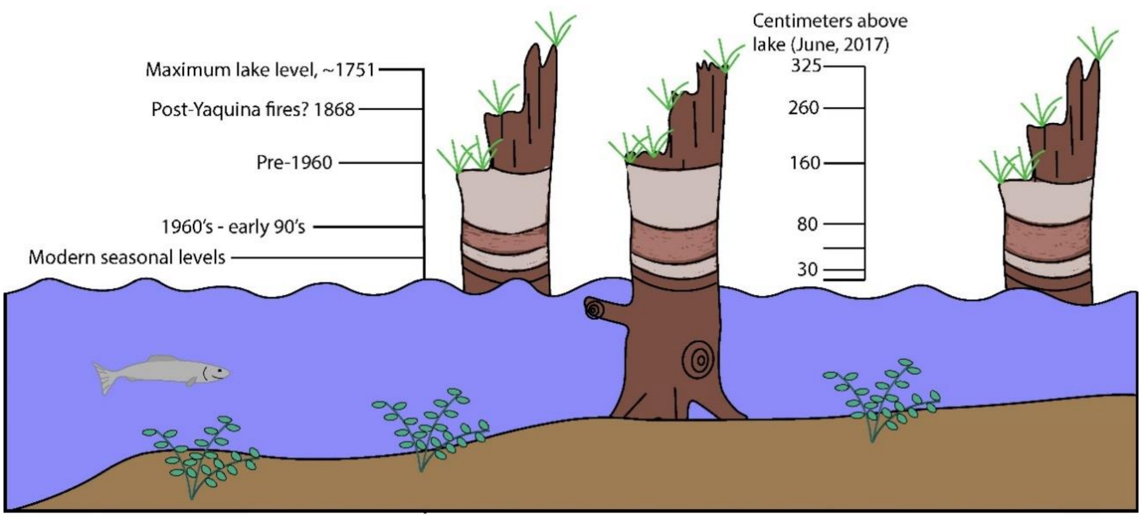

Figure 38. Simplified reconstruction of long-term changes in lake levels based on bathtub rings and weathered shelves found on drowned trees within Klickitat Lake (n=20). Maximum height of submerged trees and burned shelves indicate original lake level was over 3 m higher than present.

Evidence of a 1.6 m decrease in lake level is visible on exposed drowned Douglas-fir stumps within Klickitat Lake, while stumps in Wasson Lake are more weathered and overgrown with vegetation. Reconnaissance measurements of bathtub rings and eroded shelves of standing ghost forests within Klickitat Lake indicate that the maximum lake level was stable at approximately 3.25 m higher than today (Figure 38), correlating with the maximum height of the landslide-dam near the outlet. A series of shelves and bathtub rings on each stump in Klickitat also suggests periodic and rapid incision events followed by long-term stability. In Wasson Lake, current levels are approximately 2 m lower than the maximum height of the outlet on the landslide dam, roughly equivalent to the height of many of the trees in the lake. The weathered height of the submerged trees and similar amount of incision of the out suggest that the lake was stable after the initial formation.

Chapter V

CONCLUSION

Here I report an observed dramatic change in sedimentation regimes of the central Oregon Coast Range in the mid-20th century. The well-defined increase in sediment deposition prior to anthropogenic perturbations indicates a strong correlation in sedimentation from fluctuations in precipitation patterns and climate and secondary variability from wildfires. Anthropogenic perturbations have also had some impacts on sediment accumulation, especially when coupled with high precipitation years.

Road building and logging have affected sedimentation patterns in Klickitat and Wasson Lakes to a limited extent. Suspected human-caused lake level changes associated with alteration from the landslide dam from a downstream logging operation is the greatest contributor to increased SAR and MAR in Klickitat Lake, especially when aided by the climatic conditions in this period. The substantial lake-level decrease in the 1950s and 60s in Klickitat Lake deposited the largest volume of sediment to the basin from erosion of exposed and unvegetated slopes along the margin of the lake. Such lake level alteration through the modification of the landslide-dammed outlet instigated the progradation of deltas, affecting sediment dispersion throughout the lake. These findings suggest that landslide-dammed lakes with stable outlets are more reliable archives for deciphering the links between climate and decadal sedimentation patterns.

Changes in local climate directly affects precipitation patterns and changes in historic fire regimes but other disturbances also stimulate abrupt changes in sediment delivery and deposition. These findings indicate that the mobilization of soil and sediment in headwater hillslopes and streams can be highly variable, with minimal deposition of sediment occurring in each lake for many decades. Flood events occurred many times across the region, but many produced no change in MAR. The processes of sediment mobilization and supply within the watersheds are complex, and thus the sedimentation patterns in the lakes could not always be linked directly to single, individual events.

The study areas represent only a small part of the Tyee Formation and central Oregon Coast Range that are geomorphically altered by many processes. Sedimentation rates from other landslide-dammed lakes in the central OCR and Tyee Formation show simlar timing of sediment mobilization in the mid-20th century, but the volumes of sediment erosion and deposition are different. This variability between northern and southern lakes in the Tyee Formation (e.g. Klickitat Lake vs Wasson Lake and Loon Lake) suggest that the sediment mobilization varies across the range, with the steeper topography and debris channels of the southern Tyee Formation producing higher amounts of sediment to low-order stream channels.

REFERENCES

Appleby, P. G., and Oldfield, F. (1978). The calculation of lead-210 dates assuming a constant rate of supply of unsupported 210Pb to the sediment. *Catena*, *5*(1), 1-8.

Appleby, P. G. (2008). Three decades of dating recent sediments by fallout radionuclides: a review. *The holocene*, *18*(1), 83-93.

Baldwin, E.M., (1958). Landslide lakes in the Coast Range of Oregon: Geological Newsletter, Geological Society of the Oregon Country, v. 24, no. 4, p. 23–24.

Bartlein, P. J., Hostetler, S. W., Shafer, S. L., Holman, J. O., & Solomon, A. M. (2008). Temporal and spatial structure in a daily wildfire-start data set from the western United States (1986–96). *International Journal of Wildland Fire*, *17*(1), 8-17.

Benda, L. (1990). The influence of debris flows on channels and valley floors in the Oregon Coast Range, USA. *Earth Surface Processes and Landforms*, *15*(5), 457-466.

Benda, L., & Dunne, T. (1997). Stochastic forcing of sediment supply to channel networks from landsliding and debris flow. *Water Resources Research*, *33*(12), 2849-2863.

Beschta, R. L. (1978). Long-term patterns of sediment production following road construction and logging in the Oregon Coast Range. *Water Resources Research*, *14*(6), 1011–1016.

Blong, R. J., & Gillespie, R. (1978). Fluvially transported charcoal gives erroneous 14C ages for recent deposits. *Nature*, *271*(5647), 739.

Brown, G. W., and Krygier, J. T. (1971). Clear-Cut Logging and Sediment Production in the Oregon Coast Range. *Water Resources Research*, *7*(5), 1189-1198.

Buck C.E., Christen J.A. and James G.N. (1999). BCal: an on- line Bayesian radiocarbon calibration tool. *Internet Archaeology*, 7.

Carter, M. W., & Moghissi, A. A. (1977). Three Decades of Nuclear Testing. *Health Physics*, *33*(1), 55-71.

Cannon, S. H., Bigio, E. R., & Mine, E. (2001). A process for fire-related debris flow initiation, Cerro Grande fire, New Mexico. *Hydrological Processes*, *15*(15), 3011-3023.

Daly, C., Taylor, G. H., & Gibson, W. P. (1997). The PRISM approach to mapping precipitation and temperature. In *Proc., 10th AMS Conf. on Applied Climatology* (pp. 20-23).

Dean Jr, W. E. (1974). Determination of carbonate and organic matter in calcareous sediments and sedimentary rocks by loss on ignition: comparison with other methods. *Journal of Sedimentary Research*, *44*(1).

Deser, Clara, Trenberth, Kevin & National Center for Atmospheric Research Staff (Eds). Last modified 06 Jan 2016. "The Climate Data Guide: Pacific Decadal Oscillation (PDO): Definition and Indices." Retrieved from https://climatedataguide.ucar.edu/climate-data/pacific-decadal-oscillation-pdo-definition-and-indices.

Dibb, J. E., & Rice, D. L. (1988). Chernobyl fallout in the Chesapeake Bay region. *Journal of environmental radioactivity*, *7*(2), 193-196.

DIETRICH, W. (1978). Sediment budget for small catchment in mountainous terrain. *Zeitschrift Fur Geomorphologie, Supplementeband*, *29*, 191-206.

Eilers, J. M**.** Bernert, J. A., Gubala C. P., Whiting, M. C., Engstrom, D. R., and Charles, D. F. (1996). Recent paleolimnology of Devils Lake, Oregon. *Northwest Science* 70:13-27.

Ford, B. C., Jester, W. A., Griffith, S. M., Morse, R. A., Zall, R. R., Burgett, D. M., Bodyfelt, M. F., and Lisk, D. J. (1988). Cesium-134 and Cesium-137 in honey bees and cheese samples collected in the US after the Chernobyl accident. *Chemosphere*, *17*(6), 1153-1157.

Gilmore G, Hemingway J.D. (1995). Practical Gamma-Ray Spectrometry. Wiley: New York

Heimsath, A. M., Dietrich, W. E., Nishiizumi, K., and Finkel, R. C. (2001). Stochastic processes of soil production and transport: Erosion rates, topographic variation and cosmogenic nuclides in the Oregon Coast Range. *Earth Surface Processes and Landforms*, *26*(5), 531-552.

Heller, P. L., Peterman, Z. E., O'Neil L, J. R., & Shafiqullah, M. (1985). Isotopic provenance of sandstones from the eocene tyee formation, Oregon Coast Range. *Geological Society of America Bulletin*, *96*(6), 770-780.

Hessl, A. E., McKenzie, D., & Schellhaas, R. (2004). Drought and Pacific Decadal Oscillation linked to fire occurrence in the inland Pacific Northwest. *Ecological applications*, *14*(2), 425-442.

Hoover, L. (1963). *Geology of the Anlauf and Drain quadrangles, Douglas and Lane counties, Oregon* (No. 1122). US Government Printing Office.

Hoyt, H. M. (1966). *The good roads movement in Oregon: 1900-1920* (Doctoral dissertation, University of Oregon).

Heller, P. L., & Ryberg, P. T. (1983). Sedimentary record of subduction to forearc transition in the rotated Eocene basin of western Oregon. *Geology*, *11*(7), 380-383.

Hole, F. D. (1981). Effects of animals on soil. *Geoderma*, *25*(1-2), 75-112.

Ice, G. G., Stuart, G. W., Waide, J. B., Irland, L. C., & Ellefson, P. V. (1997). Twenty-Five Years of the Clean Water Act: How Clean Are Forest Practices?. *Journal of Forestry*, *95*(7), 9-13.

Impara, P. C. (1997). *Spatial and temporal patterns of fire in the forests of the central Oregon Coast Range* (Doctoral dissertation) Oregon State University, Oregon.

REFERENCES CONTINUED

Jackson, M., and Roering, J. J. (2009). Post-fire geomorphic response in steep, forested landscapes: Oregon Coast Range, USA. *Quaternary Science Reviews*, *28*(11), 1131-1146.

Lancaster, S. T., Hayes, S. K., & Grant, G. E. (2001). Modeling sediment and wood storage and dynamics in small mountainous watersheds. *Geomorphic processes and riverine habitat*, 85-102.

Lancaster, S. T., & Grant, G. E. (2006). Debris dams and the relief of headwater streams. *Geomorphology*, *82*(1-2), 84-97.

Lancaster, S. T., & Casebeer, N. E. (2007). Sediment storage and evacuation in headwater valleys at the transition between debris-flow and fluvial processes. *Geology*, *35*(11), 1027-1030.

Lane, J.W., (1987). *Relations between geology and mass movement features in a part of the East Fork Coquille River Watershed, Southern Coast Range, Oregon* (M.S. thesis Corvallis, Oregon State University).

Long, C. J., Whitlock, C., Bartlein, P. J., & Millspaugh, S. H. (1998). A 9000-year fire history from the Oregon Coast Range, based on a high-resolution charcoal study. *Canadian Journal of Forest Research*, *28*(5), 774-787.

Luce, C. H., & Black, T. A. (1999). Sediment production from forest roads in western Oregon. *Water Resources Research*, *35*(8), 2561-2570.

Lutz, H. J., & Griswold, F. S. (1939). The influence of tree roots on soil morphology. *American Journal of Science*, *237*(6), 389-400.

Lutz, H. J. (1960). Movement of rocks by uprooting of forest trees. *American Journal of Science*, *258*(10), 752-756.

Kelsey, H. M., Ticknor, R. L., Bockheim, J. G., & Mitchell, E. (1996). Quaternary upper plate deformation in coastal Oregon. *Geological Society of America Bulletin*, *108*(7), 843-860.

King, Tera R. and V. Bloch (2010). Lincoln County, Oregon, Community Wildfire Protection Plan. Northwest Management, Inc., Moscow, Idaho. Pp 104.

Mackey, B. H. (2009). *The contribution of large, slow-moving landslides to landscape evolution* (Doctoral dissertation, University of Oregon).

Mantua, N. J., & Hare, S. R. (2002). The Pacific decadal oscillation. *Journal of oceanography*, *58*(1), 35-44.

Marshall, J. A., & Roering, J. J. (2014). Diagenetic variation in the Oregon Coast Range: Implications for rock strength, soil production, hillslope form, and landscape evolution. *Journal of Geophysical Research: Earth Surface*, *119*(6), 1395-1417.

Marshall, J. A., Roering, J. J., Bartlein, P. J., Gavin, D. G., Granger, D. E., Rempel, A. W., ... & Hales, T. C. (2015). Frost for the trees: Did climate increase erosion in unglaciated landscapes during the late Pleistocene?. *Science advances*, *1*(10), e1500715.

Marshall, J. A., Roering, J. J., Gavin, D. G., & Granger, D. E. (2017). Late Quaternary climatic controls on erosion rates and geomorphic processes in western Oregon, USA. *GSA Bulletin*, *129*(5-6), 715-731.

Matsuoka, N. (1990). The rate of bedrock weathering by frost action: field measurements and a predictive model. *Earth Surface Processes and Landforms*, *15*(1), 73-90.

May, C. L., and Gresswell, R. E. (2003). Processes and rates of sediment and wood accumulation in headwater streams of the Oregon Coast Range, USA. *Earth Surface Processes and Landforms*, *28*(4), 409-424.

McGarigal, K., & McComb, W. C. (1995). Relationships between landscape structure and breeding birds in the Oregon Coast Range. *Ecological monographs*, *65*(3), 235-260.

Megahan, W. F., & Kidd, W. J. (1972). Effects of logging and logging roads on erosion and sediment deposition from steep terrain. *Journal of Forestry*, *70*(3), 136-141.

Morris, W. G. (1934). Forest fires in western Oregon and western Washington. *Oregon Historical Quarterly*, *35*(4), 313-339.

Morris, W. G. (1935). *The Details of the Tillamook Fire from Its Origin to the Salvage of the Killed Timber*. US Department of Agriculture, Forest Service, Pacific Northwest Forest Experiment Station.

Naiman, R. J., Johnston, C. A., & Kelley, J. C. (1988). Alteration of North American streams by beaver. *BioScience*, *38*(11), 753-762.

Nehlsen, W., Williams, J. E., & Lichatowich, J. A. (1991). Pacific salmon at the crossroads: stocks at risk from California, Oregon, Idaho, and Washington. *Fisheries, 16*(2), 4-21.

Noller, J. S. (2000). Lead-210 Geochronology. *Quaternary geochronology: methods and applications*, 115-120.

Oregon Department of Forestry Fire Inventory (2018, January). Retrieved from http://www.odf.state.or.us/DIVISIONS/protection/fire_protection/fires/FIRESlist.asp.

Olsson, I. U. (1986). Radiometric dating. In *Handbook of Holocene palaeoecology and palaeohydrology*.

Patterson III, W. A., Edwards, K. J., & Maguire, D. J. (1987). Microscopic charcoal as a fossil indicator of fire. *Quaternary Science Reviews*, *6*(1), 3-23.

Penserini, B. D. (2015). Debris flow network morphology and a new erosion rate proxy for steepland basins with application to the Oregon Coast Range and Cascadia Subduction Zone (M.S thesis, University of Oregon).

Perkins, R. W., & Thomas, C. W. (1980). Worldwide fallout. In *Transuranic elements in the environment*, 53-82.

PRISM Climate Group, Oregon State University (2017, September). Retrieved from http://prism.oregonstate.edu.

Reimer, P. J., Baillie, M. G., Bard, E., Bayliss, A., Beck, J. W., Blackwell, P. G., ... and Friedrich, M. (2009). IntCal09 and Marine09 radiocarbon age calibration curves, 0–50,000 years cal BP. *Radiocarbon*, *51*(04), 1111-1150.

Reneau, S. L., and Dietrich, W. E. (1991). Erosion rates in the southern Oregon Coast Range: Evidence for an equilibrium between hillslope erosion and sediment yield. *Earth Surface Processes and Landforms*, *16*(4), 307-322.

Richardson, K. N. D. (2017). Role of Extreme Events on Sedimentation in Loon Lake, Oregon Coast Range, USA (unpublished master's thesis). Oregon State University, Oregon.

Roering, J. J., Kirchner, J. W., & Dietrich, W. E. (1999). Evidence for nonlinear, diffusive sediment transport on hillslopes and implications for landscape morphology. *Water Resources Research*, *35*(3), 853-870.

Roering, J. J., Kirchner, J. W., and Dietrich, W. E. (2005). Characterizing structural and lithologic controls on deep-seated landsliding: Implications for topographic relief and landscape evolution in the Oregon Coast Range, USA. *Geological Society of America Bulletin*, *117*(5-6), 654-668.

Rummery, T. A. (1983). The use of magnetic measurements in interpreting the fire histories of lake drainage basins. *Hydrobiologia*, *103*(1), 53-58.

Snavely, P. D., Wagner, H. C., & MacLeod, N. S. (1964). Rhythmic-bedded eugeosynclinal deposits of the Tyee formation, Oregon Coast Range. *Kansas Geological Survey Bulletin*, *169*, 461-480.

Swanson, F. J., and Dyrness, C. T. (1975). Impact of clear-cutting and road construction on soil erosion by landslides in the western Cascade Range, Oregon. *Geology*, *3*(7), 393-396.

Swanston, D. N., & Swanson, F. J. (1976). Timber harvesting, mass erosion, and steepland forest geomorphology in the Pacific Northwest. *Geomorphology and engineering*, *4*, 199-221.

Swanson, F. J., Fredriksen,R. L., and McCorison, F. M., (1982). *Material transfer in a western Oregon forested watershed*, Edmonds, R. L., ed., Analysis of coniferous forest ecosystems in the western United States: Stroudsburg, Pennsylvania, Hutchison Ross Publishing, 233–266.

Telford, R. J., Heegaard, E., & Birks, H. J. B. (2004). All age–depth models are wrong: but how badly?. *Quaternary science reviews*, *23*(1-2), 1-5.

Thompson, R., & Oldfield, F. (1986). *Environmental magnetism*. London: Allen and Unwin.

Walker, G.W. and MacLeod, N.S., (1991). Geologic map of Oregon: U.S. Geological Survey, scale 1:500,000

Walker, M., & Walker, M. J. C. (2005). *Quaternary dating methods*. John Wiley and Sons.

Watson, R., & Oregon State Highway Commission. (1951). *Casual and factual glimpses at the beginning and development of Oregon's roads and highways*. Salem, Or: Oregon State Highway Commission.

Western Regional Climate data, (2017). Retrieved from https://www.wrcc.dri.edu

Wheatcroft, R. A., Goñi, M. A., Richardson, K. N., & Borgeld, J. C. (2013). Natural and human impacts on centennial sediment accumulation patterns on the Umpqua River margin, Oregon. *Marine Geology*, *339*, 44-56.

Whitlock, C., & Millspaugh, S. H. (1996). Testing the assumptions of fire-history studies: an examination of modern charcoal accumulation in Yellowstone National Park, USA. *The Holocene*, *6*(1), 7-15.

Whitlock, C., & Larsen, C. (2002). Charcoal as a fire proxy. In *Tracking environmental change using lake sediments* (pp. 75-97). Springer, Dordrecht.

Wilson, C. J., Carey, J. W., Beeson, P. C., Gard, M. O., & Lane, L. J. (2001). A GIS-based hillslope erosion and sediment delivery model and its application in the Cerro Grande burn area. *Hydrological Processes*, *15*(15), 2995-3010.

Worona, M. A., & Whitlock, C. (1995). Late quaternary vegetation and climate history near Little Lake, central Coast Range, Oregon. *Geological Society of America Bulletin*, *107*(7), 867-876.

Yamamoto, M., Kofugi, H., Shiraishi, K., & Igarashi, Y. (1998). An attempt to evaluate dry deposition velocity of airborne210Pb in a forest ecosystem. *Journal of radioanalytical and nuclear chemistry*, *227*(1-2), 81-88.

Zybach, B. (2003). The great fires: Indian burning and catastrophic forest fire patterns of the Oregon Coast Range, 1491-1951.